SECURITY CLASSIFICATION OF THIS PAGE

REPORT DOCUMENTATION PAGE

1a. REPORT SECURITY CLASSIFICATION UNCLASSIFIED	1b. RESTRICTIVE MARKINGS
2a. SECURITY CLASSIFICATION AUTHORITY	3. DISTRIBUTION / AVAILABILITY OF REPORT Approved for public release; distribution unlimited.
2b. DECLASSIFICATION / DOWNGRADING SCHEDULE	
4. PERFORMING ORGANIZATION REPORT NUMBER(S) NRL Memorandum Report 6076	5. MONITORING ORGANIZATION REPORT NUMBER(S)
6a. NAME OF PERFORMING ORGANIZATION Naval Research Laboratory 6b. OFFICE SYMBOL (*If applicable*) Code 8320	7a. NAME OF MONITORING ORGANIZATION
6c. ADDRESS (*City, State, and ZIP Code*) Washington, DC 20375-5000	7b. ADDRESS (*City, State, and ZIP Code*)
8a. NAME OF FUNDING / SPONSORING ORGANIZATION SPAWAR (PMW-142-2) 8b. OFFICE SYMBOL (*If applicable*)	9. PROCUREMENT INSTRUMENT IDENTIFICATION NUMBER
8c. ADDRESS (*City, State, and ZIP Code*) Space and Naval Warfare Systems Command Washington, DC 20363-5100	10. SOURCE OF FUNDING NUMBERS PROGRAM ELEMENT NO. 64777N; PROJECT NO.; TASK NO. x0699; WORK UNIT ACCESSION NO. 83-0733-0

11. TITLE (*Include Security Classification*)
On-Orbit Frequency Stability Analysis of the GPS NAVSTAR 8 Rubidium Clock and NAVSTARs 9 and 10 Cesium Clocks

12. PERSONAL AUTHOR(S) Buisson, James A. and Largay, Marie M.

13a. TYPE OF REPORT	13b. TIME COVERED	14. DATE OF REPORT (*Year, Month, Day*)	15. PAGE COUNT
Memorandum Report	FROM Jan '85 TO Dec '85	1987 September 17	52

16. SUPPLEMENTARY NOTATION

17. COSATI CODES		
FIELD	GROUP	SUB-GROUP

18. SUBJECT TERMS (*Continue on reverse if necessary and identify by block number*)
NAVSTAR; Frequency stability; Cesium clock; Global Positioning System (GPS); Rubidium clock; Allan variance

19. ABSTRACT (*Continue on reverse if necessary and identify by block number*)

This report describes the on-orbit frequency stability performance analysis of the Global Positioning System (GPS) NAVSTAR 8 rubidium clock and the NAVSTARs 9 and 10 cesium clocks. Time domain measurements, taken from three GPS monitor sites and from the United States Naval Observatory (USNO), have been analyzed to determine the short and long-term frequency stability performance of the NAVSTAR clocks. The data presented include measurements from 1985.

20. DISTRIBUTION / AVAILABILITY OF ABSTRACT ☒ UNCLASSIFIED/UNLIMITED ☐ SAME AS RPT. ☐ DTIC USERS	21. ABSTRACT SECURITY CLASSIFICATION UNCLASSIFIED
22a. NAME OF RESPONSIBLE INDIVIDUAL Marie M. Largay	22b. TELEPHONE (*Include Area Code*) (202)767-2595 22c. OFFICE SYMBOL Code 8320

DD FORM 1473, 84 MAR 83 APR edition may be used until exhausted. All other editions are obsolete

SECURITY CLASSIFICATION OF THIS PAGE

*U.S. Government Printing Office: 1985—507-047

18. SUBJECT TERMS (Continued)

Interim Control Segment (ICS)
Weighted ensemble
Clock analysis

Naval Research Laboratory
Washington, DC 20375-5000

NRL Memorandum Report 6076

On-Orbit Frequency Stability Analysis of the GPS NAVSTAR 8 Rubidium Clock and NAVSTARs 9 and 10 Cesium Clocks

MARIE M. LARGAY AND JAMES A. BUISSON

Space Applications Branch
Space Systems Technology Department

September 17, 1987

CONTENTS

ON-ORBIT FREQUENCY STABILITY ANALYSIS OF THE GPS NAVSTAR 8 RUBIDIUM CLOCK AND NAVSTARs 9 AND 10 CESIUM CLOCKS

INTRODUCTION

The NAVSTAR Global Positioning System (GPS) is a Department of Defense (DOD) space-based satellite system. When operational 18 satellites in six orbital planes will provide accurate navigation information to users anywhere in the world. Examples of GPS use are point-to-point navigation, search/rescue operations, and passive rendezvous. GPS can provide navigational updates to platforms with other navigational systems.

A role of the Naval Research Laboratory (NRL) in GPS is to develop space-qualified atomic clocks for use in the NAVSTAR spacecraft. This includes pre-flight and post-flight frequency stability analyses [1,2] to ensure that on-orbit accuracy and stability requirements are met [3].

This report summarizes the on-orbit frequency stability analysis of the GPS NAVSTAR 8 rubidium clock and the GPS NAVSTARs 9 and 10 cesium clocks. Reference 3 summarized the results of the frequency stability of the clocks on-board NAVSTARs 3, 4, 5, and 6. The official termination of the Interim Control Segment (ICS) of GPS occurred on September 15, 1985 (day 258). This report concludes the performance analysis of the clocks on-board all operational NAVSTARs using data from the ICS system.

Time domain measurements, taken from the ICS Monitor Sites (MS) and from the United States Naval Observatory (USNO), have been analyzed to estimate the frequency stability performance of the NAVSTAR clocks. The frequency stability results include both short-term (sample times of 900 to 7200 seconds) and long-term (sample times of 1 to 10 days and 10 to 30 days). Results are

Manuscript approved June 9, 1987.

shown for data collected at the ICS MSs for the year 1985 (through day 258) and at USNO for the entire year.

GPS SYSTEM DESCRIPTION

The NAVSTAR GPS system is mainly comprised of the Control and Space segments:

(a) Control Segment

The ICS consisted of a Master Control Station (MCS), located at Vandenberg, California, and four monitor sites located at Vandenberg, Hawaii, Alaska, and Guam. These four monitor sites tracked the GPS space vehicles (SV). Data from these sites were transmitted to the MCS and processed to determine SV orbits and clock errors. Separate facilities were used for command and telemetry information, and to upload navigational data to the SV [3].

(b) Space Segment

During the period covered in this report, the Space Segment consisted of a constellation of eight NAVSTAR SVs. Each SV contains multiple clocks. The launch dates and the clock used are detailed in Table 1:

Table 1 - Launch Dates and Frequency Standard Type of NAVSTAR SVs

GPS SV	LAUNCH TIME	CURRENT FREQUENCY STANDARD
NAVSTAR 1	2-22-78	QUARTZ
NAVSTAR 3	10-07-78	RUBIDIUM
NAVSTAR 4	12-11-78	RUBIDIUM
NAVSTAR 6	4-26-80	RUBIDIUM
NAVSTAR 8	7-14-83	RUBIDIUM
NAVSTAR 9	9-10-84	CESIUM
NAVSTAR 10	10-09-85	CESIUM

Each SV continuously broadcasts spread spectrum signals that are generated from the on-board clock. The navigation (NAV)

message is modulated onto the signal with data which defines GPS time.

The "precise," or P-code, modulation is transmitted at two frequencies in the L-band (1227.6 and 1575.42 MHz). These are designated as L_1 and L_2 signals, and are modulated at 10.23 Mbps (million bits per second). The P-code modulation provides the capability for high precision time difference measurements, is resistant to electronic countermeasures (ECM) and is denied to unauthorized users by means of transmission security devices. The P-code employs a very long pseudo-random code that is reset once per week. The second code which is designated as the coarse/acquisition code (C/A) is modulated at 1.023 Mbps, repeats every millisecond and is transmitted on L_1. It provides a coarse signal that is a factor of ten less precise than the P-code. It is used for navigation that is less precise, and serves as an acquisition aid for authorized users to gain access to the P-signal. Each SV broadcasts at the same nominal frequency. The use of the spread spectrum modulation and separate codes permits multiple access to any of the satellites that are above the user's horizon [2,3].

In operational use, a navigational solution is obtained from simultaneous measurements from four SVs of apparent time difference. These measurements are called pseudo-ranges (PR) because SV or user clock errors will cause apparent range errors. The time differences are taken between the user receiver clock and each of the SV clocks. Using a computer-controlled receiver, a user tunes and locks the receiver to the SV signals, and makes four simultaneous pseudo-ranges. The four SV positions are calculated from the NAV message. When the system is fully operational at least four SVs will be in view of the user anywhere on earth. The four PR are used to calculate the user's latitude, longitude, height, and clock offset [4,5]. With the development SVs shown in Table 1, they are arranged to provide periods of four SV visibility over the principal test range at Yuma, Arizona.

A solution for the user's velocity may be computed by simultaneous measurements of apparent frequency difference or Doppler. These measurements are called pseudo-range-rate (PR-rate). Basic navigation for user position and clock error is independent of the user's velocity [3].

ON-ORBIT CLOCK ANALYSIS

The instantaneous navigation capability is possible because each SV clock is synchronized to a common time. The clock error offset, orbital elements, and spacecraft health parameters of all SVs in the constellation are continuously monitored and determined at the MCS. They are used to generate the NAV message, which are uploaded to each SV. Each SV clock must then maintain time until the next clock prediction update.

A technique for analyzing time/frequency stability of orbiting clocks and frequency standards was developed in 1975 [6,7]. This technique has evolved into an analytical procedure depicted in Fig. 1. Each major component of the frequency stability analyses is described in this report.

FREQUENCY STABILITY MODEL

The Allan variance is used to estimate frequency stability. The calculation requires that four quantities be specified: N (the number of frequency samples, denoted by y), T (the measurement repetition interval of duration τ), τ (the sample time), and f_h (the system noise bandwidth). The standard deviation of the frequency fluctuations, $\sigma_y(\tau)$ is shown below in Eq. (1):

$$\sigma_y^2(\tau) = \sigma_y^2(N=2,\ T=\tau,\ \tau, f_h) = \left\langle \frac{(\bar{y}_{k+1} - \bar{y}_k)^2}{2} \right\rangle \qquad (1)$$

The bar over the y indicates the time average over the interval τ; the angular brackets indicate the time average of the

quantity. The computational form used in this analysis differs from Eq. (1) and is given by Eq. (2), where M denotes the frequency samples with sample period T equal to the sampling time, τ: [8,9]

$$\sigma_y^2(\tau) = \frac{1}{(M-1)} \sum_{k=1}^{M-1} \frac{(\bar{y}_{k+1} - \bar{y}_k)^2}{2} \qquad (2)$$

The average frequency, $\bar{y}_k$, calculated from pairs of clock offsets, Δt, separated by sample time, τ, are given by:

$$\bar{y}_K = \frac{\Delta t_{k+1} - \Delta t_k}{\tau} \qquad (3)$$

The clock offsets are estimated from the SV pseudo-ranges [2,6].

CLOCK DIFFERENCE MEASUREMENTS

The PR and integrated PR-rate data are taken between the SV and MS clocks by the MCS and MS. The MS receivers are capable of receiving all SVs in view simultaneously. The PR are taken once every 6 seconds and then corrected for known errors and smoothed to produce a 15-minute value. The corrections are for equipment delay, ionospheric delay, tropospheric delay, earth rotation, and relativistic effects. Then the data are edited and smoothed using the predicted SV ephemeris to calculate the geometric range delay. The clock offset at the midpoint of the 15-minute data span is estimated by using both PR and PR-rate measurements, which are fitted to a cubic polynomial with epoch at the time corresponding to the midpoint of the data.

The equation that relates the pseudo-range measurements to the clock difference between NAVSTAR SV and the MS is:

$$PR = R + C(t_{MS} - t_{SV}) + C\Delta t_A + \varepsilon \qquad (4)$$

where:

PR = the measured pseudo-range
R = the slant, or geometric range, from the SV (at the time of transmission) to the MS (at the time of reception)
C = the speed of light
t_{MS} = the MS clock time of transmission
t_{SV} = the SV clock time at reception
t_A = ionospheric, tropospheric, and relativistic delay, with corrections for antenna and equipment delays
ε = the measurement error

The clock difference, denoted by Δt_k for the k^{th} measurement, is obtained by rearranging Eq. (4) into

$$\Delta t_k = (t_{SV} - t_{MS}) = R_k/C + \Delta t_A + \varepsilon/C - PR_k/C \quad (5)$$

ORBIT ESTIMATION

All of the pseudo-range data from the four MSs are collected at the MCS. These data are processed to produce a current and predicted estimate of each of the SV clock and ephemeris states. These data are further processed to produce a post-flight estimate of the SV ephemerides.

The current and predicted estimates of the SV clock and ephemeris states are made using a Kalman [10,11,12] estimator. The success of the estimation is highly dependent on the stability of the SV and MS clocks. If the SV clock does not meet a maximum clock uncertainty of about 5 nanoseconds during the pass, then the Kalman estimator has difficulty in separating the orbit part of the GPS signal from the clock noise. Equation (5) shows that the MS clock has the same weight in the measurement as the SV clock. It is therefore highly desirable to have an MS clock of equal or better time stability than the SV clock at each MS [3].

Determination of the SV orbits are routinely made by the Naval Surface Weapons Center (NSWC). They use an orbit estimation program [13] that extensively models the dynamics of the satellite motion, including solar radiation pressure, pole wander, earth tides, and orbit adjust maneuvers. The orbits are made once per week using all available observations for a two-week span from each of the MS.

The purpose of precise orbit estimation for this analysis is to separate the clock and orbital components. That process models the clock as a constant, but unknown, frequency. The clock model includes an aging rate, which may be used for frequency standards that exhibit aging. The model also is capable of segmenting the clock bias solution to allow for frequency adjustments of the MS or SV clock.

CLOCK DIFFERENCE DATA

The clock differences used for analyzing the SV clock as discussed in this report incorporate the post-flight orbital positions and the 15-minute PR to calculate the clock differences according to Eq. (5). The clock differences for each pass are then used to estimate the clock differences at the time-of-closest-approach (TCA) of the SV over the MS. This procedure results in either one or two points per day, depending on the orbit and the MS location.

The evaluation of the clock difference at TCA minimizes the effect of the orbital position estimate for along-track and out-of-plane errors. This procedure does not reduce the effect of radial SV orbit position errors. Therefore, the radial error will be one of the factors that limits the long-term frequency stability analysis. Other factors include residual correction effect from the pre-processing of the 15-minute data, ionospheric effects, and system noise sources.

USNO DATA

The USNO also tracks the SVs. Rather than using a single cesium standard as a signal reference, the master clock at USNO driven by an ensemble of cesium clocks, is used. The USNO receiver is only capable of taking C/A data at L_1 only. The C/A PR are taken at 6 second intervals, aggregated and smoothed every 13 minutes. The satellite ephemeris used is from the transmitted predicted NAV message. The ionospheric delays are compensated for by the ionospheric model parameters contained in the NAV message.

The clock-difference data received from USNO includes a single point representing a 13-minute data collection per SV pass. USNO does not track all SVs from horizon-to-horizon. Specific SVs are tracked at the same time that other ground stations are tracking in order to obtain simulatenous data for common-view measurements. The USNO data is sorted by SV into data files and a single TCA point chosen for each day.

LONG-TERM FREQUENCY STABILITY

The long-term frequency stability analysis performed utilized data from the four ICS MSs (Vandenberg, Hawaii, Alaska and Guam) and from USNO. The MCS Daily reports and the clock difference data were analyzed to determine any discontinuities and the possible causes for them. The Guam MS data was too erratic to calculate the frequency stability. Many communication link down-times, maintenance down-times, and power outages resulted in considerable missing data and many discontinuities. Figure 2 is the data between Guam and NAVSTAR 8 for 1985. Consequently, the Guam data was not used. Discontinuities in the data from Vandenberg MS, Hawaii MS, Alaska MS, and USNO, and possible causes are delineated in Table 2.

Table 2 - Discontinuities in Clock Difference Data, 1985

SV RELATED

NAVSTAR 8

Day of Year	Possible Cause
134	Time Steering* went into effect
157	2 Z-adjusts**
209	Annual Clock Maintenance of on-board cesium
361	Phase Shift***

NAVSTAR 9

Day of Year	Possible Cause
65	2 Z-adjusts
297	Phase Shift

NAVSTAR 10

NONE

MS RELATED

MS	Day of Year	Possible Cause
Hawaii	172	Down for maintenance
Hawaii	198	Phase Shift
USNO	245	Break in data for NAVSTAR 8

*Time Steering - the continuous correction of GPS time to keep it within +/- 1 microsecond of UTC (USNO).

**Z-adjust - a reset of SV clock frequency to stay within offset limits of $+/- 1 \times 10^{12}$.

***Phase Shift - unexplained discontinuity

The Time Steering that went into effect on day 134 did not affect NAVSTARs 9 and 10. However, NAVSTAR 8 data had an apparent discernible discontinuity at that time. It is not conclusive that time steering created this problem, but other causes have not been identified.

A second degree fit to each SV pass was used to compensate for residual PR errors before analyzing the frequency stability. The clock behavior values, which is expressed by Eq. 6, of phase (a_0) and frequency (a_1) coefficients were also calculated. The aging (a_2) or drift coefficient is large for the rubidium clock on-board NAVSTAR 8, in comparison to the cesium clocks on-board NAVSTARS 9 and 10. This is expected since a characteristic of cesium frequency standards is no appreciable aging (See Table 3).
The clock difference data was segmented at the data discontinuities, and a second degree fit made to each of these segments, solving for the a_0, a_1, and a_2 coefficients. The epoch is the midpoint of the data span, which is denoted by START and STOP.

Table 3 - Coefficients (a_0, a_1, a_2)

EPOCH (Day)	PHASE (μs)	FREQUENCY (PP10(13))	AGING (PP10(13)/day)	START (Day)	STOP (Day)
NAVSTAR 8 (Rubidium)					
Vandenberg MS					
66.	630.785	574.138	-2.155	1.00000	134.99999
146.	968.407	406.979	-1.983	135.00000	157.99999
183.	190.337	332.933	-2.008	158.00000	209.99999
234.	165.561	237.275	-1.896	210.00000	258.99999
average aging -2.010 PP10(13)/day					
Hawaii MS					
68.	61749.038	544.627	-2.175	3.00000	134.99999
146.	62059.748	381.337	-2.147	135.00000	157.99999
165.	61222.725	341.585	-2.124	158.00000	172.99999
185.	67980.791	302.979	-2.017	173.00000	198.99999
204.	68755.391	267.302	-1.813	199.00000	209.99999
221.	68642.259	235.800	-1.774	210.00000	232.99999
average aging -2.008 PP10(13)/day					
Alaska MS					
73.	63092.010	529.275	-2.171	12.00000	134.99999
146.	63376.619	376.703	-2.003	135.00000	157.99999
183.	62588.733	302.628	-1.963	158.00000	209.99999
233.	62548.763	208.878	-1.808	210.00000	257.99999
average aging -1.986 PP10(13)/day					
USNO					
67.	-545.381	-547.357	2.163	1.00000	134.99999
146.	-861.403	-381.970	2.076	135.00000	157.99999
183.	- 75.042	-307.043	1.990	158.00000	208.99999
227.	- 25.599	-224.389	1.784	209.00000	245.99999
305.	-130.608	- 90.980	1.613	246.00000	361.99999
363.	-150.971	- 0.568	1.164	362.00000	365.99999
average aging +1.925 PP10(13)/day					

NAVSTAR 9 (Cesium)
Vandenberg MS

EPOCH (Day)	PHASE (μs)	FREQUENCY (PP10(13))	AGING (PP10(13)/day)	START (Day)	STOP (Day)
39.	20.912	50.772	.037	14.00000	65.99999
161.	72.689	50.057	.012	66.00000	257.99999
Hawaii MS					
40.	61135.773	26.514	-.003	15.00000	65.99999
119.	61151.827	24.009	-.012	66.00000	172.99999
185.	67867.798	24.955	.043	173.00000	198.99999
216.	68602.535	25.703	.000	199.00000	232.99999
Alaska MS					
38.	62456.353	22.174	-.001	14.00000	64.99999
161.	62476.862	19.959	.008	65.00000	257.99999
USNO					
39.	63.512	-26.542	-.020	14.00000	64.99999
181.	33.495	-24.890	.000	65.00000	297.99999
333.	-5.716	-23.428	-.001	298.00000	365.99999

NAVSTAR 10 (Cesium)
Vandenberg MS

EPOCH (Day)	PHASE (μs)	FREQUENCY (PP10(13))	AGING (PP10(13)/day)	START (Day)	STOP (Day)
128.	230.411	88.061	-.003	1.00000	258.99999
Hawaii MS					
88.	61303.918	62.920	-.013	3.00000	172.99999
185.	68058.579	62.247	.008	173.00000	198.99999
214.	68802.102	61.736	-.087	199.00000	230.99999
Alaska MS					
133.	62645.705	58.036	-.013	12.00000	255.99999
USNO					
183.	-156.858	-62.042	.019	2.00000	365.99999

After these coefficients are determined, they are used in the equation;

$$\Delta t_{ADJ} = a_0 + a_1 \Delta t_{DIFF} + \frac{1}{2} a_2 \Delta t_{DIFF}^2 \qquad (6)$$

where Δt_{DIFF} = time difference between the epoch and a given data point

Δt_{ADJ} = adjustment to the clock difference

This adjustment (Δt_{ADJ}) is then applied to the clock difference resulting in a "corrected" value for clock difference (Eq. (7)). This compensates for discontinuities in phase, frequency, and aging;

$$\Delta t_{COR} = \Delta t_K - \Delta t_{ADJ} \tag{7}$$

where Δt_{COR} is the "corrected" value for clock difference

NAVSTAR 8 RESULTS

The long-term frequency stability of the rubidium clock on-board NAVSTAR 8 was determined using two methods. The results are drastically different.

First, "corrected" values for the clock differences were calculated using the coefficients (a_0, a_1, and a_2) for each of the segments described above. The frequency stability was determined using these "corrected" clock differences. Figures 3 and 4 demonstrate the results using data from Vandenberg, Hawaii, Alaska, and USNO.

Since each MS uses one clock as a reference, to provide a common reference for each SV, a weighted ensemble, using the $\sigma_y(\tau)$ values from the MSs, is calculated. This weighted ensemble will better represent the SV clock performance, because individual MS performance phenomenon will not be as prominent. The weighted ensemble $\sigma_y(\tau)$ values were calculated using the results from the three MS. The equation for calculating the weighted average of the variance (σ_w^2) follows;

$$\sigma_w^2 = \frac{N_V\sigma_V^2 + N_H\sigma_H^2 + N_A\sigma_A^2}{N_V + N_H + N_A} \tag{8}$$

where: V, H, A is from the respective MS
N = number of data points from each MS.

The weighted ensemble and USNO results are shown in Fig. 5. It can be seen that these results are almost identical. Using the ensemble of clocks at USNO and using a MS weighted ensemble, each using a single ground clock, produces similar frequency stability results. This result will be addressed later in the report.

The second method applied the aging term differently. "Corrected" values for the clock differences were calculated using the segmented coefficients for a_0 and a_1 (phase and frequency) and one average value for a_2 (aging) for the year. The frequency stability was calculated using these "corrected" clock differences.

This method used the MS and USNO data in the same fashion as the first method. The results of which is shown in Figs. 6 and 7. The weighted ensemble values were calculated and Fig. 8 demonstrates again how closely the USNO and weighted ensemble results agree.

The frequency stability results depending on whether the segmented values for aging are used, or one average value for aging is used, vary greatly. The method of handling the aging coefficient is critical to estmating rubidium clock performance as shown by comparing Figs. 5 and 8. The rate of change of the aging is so large, that using one average value for the time span produces incorrect frequency stability estimates. These results show that using a rubidium clock, like that on-board NAVSTAR 8, would be difficult for long-term operations without corrections. During long-term operations without upload of new PR corrections and SV trajectory, the SV position and clock coefficients would be predicted for this period. Since the rubidium clock does not have a fixed or constant aging rate, and any changes of aging rates are not accurately known until after the fact, this clock would not support accurate data without correction for long-term operations.

NAVSTAR 9 RESULTS

The long-term frequency stability of the cesium clock on-board NAVSTAR 9 was estimated initially without correcting for the coefficients for phase, frequency, and aging. If there were no discontinuities in the data, this method would be preferred since the aging associated with the cesium clock is very small. However, since there were obvious system (Table 2) and other discontinuities, that method is not realistic.

The frequency stability was estimated using the "corrected" clock differences, applying the coefficients (a_0, a_1, a_2), as determined for each segment between discontinuities. The coefficients for phase and frequency were necessary to compensate for the discontinuities. Figures 9 and 10 show the results from the MSs and USNO. The MS weighted ensemble values were calculated, and Fig. 11 exhibits how closely the results compare with USNO.

NAVSTAR 10 RESULTS

The long-term frequency stability of the cesium clock on-board NAVSTAR 10 was determined using two methods. Initially, the frequency stability was estimated without correcting for phase, frequency, or aging. The data from all of the MSs, except Hawaii, was very smooth with no discontinuities. As described in Table 2, Hawaii had two discontinuities; one on day 172 when the station was down for maintenance and on day 198, when a gross shift in phase (730μs) occurred. The frequency stability results bridging these segments were so large that they were automatically filtered.

Secondly, the coefficients for phase, frequency, and aging were determined and "corrected" clock differences were calculated. The frequency stability was re-calculated. As expected with a cesium clock, the aging term was extremely small. Due to the small aging and smooth data, the removal of the

coefficients had very little effect in the frequency stability results. Figures 12 through 15 show the results using both methods. Slight aging can be noted as the sample time, τ, increases in the very long-term (τ = 20 days).

The weighted ensemble values were calculated, correcting for phase, frequency, and aging. Figure 16 demonstrates the comparison of the frequency stability results using USNO and weighted ensemble data.

SHORT-TERM FREQUENCY STABILITY

In addition to the long-term (one day or greater) frequency stability, analysis has been performed using the individual PR obtained at 15-minute intervals. These data are at the MCS sampling time and were examined as to clock stability over the duration of an individual pass. The short-term frequency stability was calculated using all of the 1985 data from the MSs on NAVSTARs 8, 9, and 10. Data was not available from USNO to calculate the short-term frequency stability since that data is not taken from horizon-to-horizon on all passes. The short-term frequency stability was calculated for sample times, τ, of 900, 1800, 2700, 3600, 4500, 5400, 6300, and 7200 seconds within a pass. The results are displayed in Figs. 17 through 19 for NAVSTARS 8, 9, and 10 respectively.

Two other types of plots are used to more fully explain the short-term frequency stability results. The first type presents the $\sigma_y(\tau)$ averaged over consecutive 5-day sets [3], as a function of time of year. A separate plot is made for each of the eight sample times. Figure 20 is a sample of this plot from Vandenberg MS using NAVSTAR 8 data. The second type of plot shows a value for every $\sigma_y(\tau)$ for each of the eight sample times. This type is very helpful in discovering problem areas, major outliers, or trends in on-orbit clock performance. Figure 21 is a sample of this type of plot from Vandenberg MS using NAVSTAR 8 data.

SUMMARY

The $\sigma_y(\tau)$ weighted ensembles that were calculated for 1985 for both short-term and long-term frequency stability are shown in Figs. 22 through 24. The long-term results have the segmented discontinuities included with the corrections for phase, frequency, and aging. Confidence limits were calculated for the $\sigma_y(\tau)$ values. Due to the large number of samples in our data, the confidence limits were very small. A sample of these results for NAVSTAR 8 using Vandenberg MS data is shown in Fig. 25.

All of the long-term frequency stability results have been calculated for sample times, τ, ranging from 1 to 10 days and from 10 to 30 days. In practice, it is desirable to have a data base length which is at least ten times larger than the sample time. In this report, the results presented for the ICS MS include data for days 1 through 258; the results for USNO include data for days 1 through 365. Therefore, a sample time, τ, of 30 days is the maximum allowable sample time. The results for NAVSTARs 8, 9, and 10 from USNO and the calculated weighted ICS ensemble compare very well through a sample time of 30 days. The differences in the data collection techniques between USNO and the ICS MSs are summarized in Fig. 26. This shows the different methods used for measuring parameters as has been described in detail previously. The data NRL receives from the MCS from the four MSs measures dual frequency, whereas USNO measures single frequency. The ground clock at each MS is a single cesium. USNO has an ensemble of clocks. The satellite ephemeris used by NRL is the NSWC post-flight fit; USNO receives the values from the predicted NAV message. The data rate/pass is also different, as shown in Fig. 26.

As shown in Figs. 5, 8, 11 and 16, the frequency stability results using data from USNO and the weighted ICS ensemble are almost identical. An added benefit to processing the ICS MS data is that the the individual ground station's performance as well as the performance of their ground clock can be analyzed.

Anomalies can be detected that are peculiar to the ground stations.

Once a clock has been characterized through a frequency stability analysis, the frequency stability may then be used to estimate a clock's time prediction performance. A set of time prediction curves is presented by Fig. 27, as a function of frequency stability and clock update time, using an optimal two point prediction. This algorithm and other models for estimating time stability are presented in reference 8. Each of these time prediction models has one thing in common, namely that the long-term clock prediction performance is driven by the product of the clock update time and the frequency stability. Therefore, the frequency stability is a fundamental measure of time prediction performance, or time stability. The length of time between NAVSTAR clock updates is determined by overall system performance, hence, improved frequency stability (clock stability) is the parameter that will directly influence GPS time prediction [14].

The short-term and long-term frequency stability results for NAVSTARs 8, 9, and 10 are summarized in Fig. 28. The GPS Block I specifications are shown in this plot. The summary shows the performance of the NAVSTAR 8 rubidium clock and the NAVSTARs 9 and 10 cesium clocks are not within GPS specifications in the short-term. At the one day point, NAVSTAR 8 and 9 appear to be on or slightly above specification. All appear to be under specification in the long-term.

ACKNOWLEDGEMENTS

The authors acknowledge Thomas B. McCaskill and Sarah B. Stebbins for technical consultation, and Frances Wright and Bettejean McKnight for manuscript preparation. Acknowledgements are also given to Clarence Carson of the Bendix Corporation for his assistance in processing the data.

REFERENCES

1. C.A. Bartholomew, "Satellite Frequency Standards," Nav.: J. of the Inst. of Nav. 25(2), Summer 1978, pp. 113-120.

2. T.B. McCaskill, S.B. Stebbins, C.E. Carson, and J.A. Buisson, "Long Term Frequency Stability Analysis of the GPS NAVSTAR-6 Cesium Clock," NRL Report 8599, Sept. 1982.

3. T.B. McCaskill, J.A. Buisson, and S.B. Stebbins, "Frequency Stabilty Analysis of GPS NAVSTARs 3 and 4 Rubidium Clocks and the NAVSTARs 5 and 6 Cesium Clocks," NRL Report 8778, Dec. 1983.

4. J.A. Buisson and T.B. McCaskill, "TIMATION Navigation Satellite System Constellation Study," NRL Report 7389, June 1972.

5. T.B. McCaskill, J.A. Buisson, and D.W. Lynch, "Principles and Techniques of Satellite Navigation Using the TIMATION II Satellite," NRL Report 7252, June 1971.

6. T.B. McCaskill and J.A. Buisson, "NTS-1 (TIMATION III) Quartz- and Rubidium-Oscillator Frequency-Stability Results," NRL Report 7932, Dec. 1975.

7. J.A. Buisson, T.B. McCaskill, O.J. Oaks, M.M. Largay, S.B. Stebbins, "GPS NAVSTAR-4 and NTS-2 Long Term Frequency Stability and Time Transfer Analysis," NRL Report 8419, June 1980.

8. David W. Allan, et al., "Statistics of Time and Frequency Data Analysis," NBS Monograph 140,"TIME and FREQUENCY: Theory and Fundamentals," Chap. 8, May 1974.

9. David W. Allan, "Statistics of Atomic Frequency Standards," Proc. IEEE, 54(2), Feb. 1966, pp. 221-230.

10. R.E. Kalman, "A New Approach to Linear Filtering and Prediction Problems," Trans. ASM Eng. J. Basic Eng. Series D, 82, Mar. 1960, pp. 35-45.

11. Bernard Friedland, "A Review of Recursive Filtering Algorithms," Proc. of the Spring Joint Comp. Conf., AFIPS Conference Proc. 40 1972, pp. 163-180.

12. S.S. Russell and J.H. Schaibly, "Control Segment and User Performance," J. of The Inst. of Nav., 25 (6), Summer 1978, pp. 166-172.

13. J.W. O'Toole, "CELEST Computer Program for Computing Satellite Orbits," NSW/DL TR 3565, Oct. 1976.

14. T.B. McCaskill and J.A. Buisson, "On-Orbit Frequency Stability Analysis of NAVSTAR GPS Clocks and the Importance

of Frequency Stability to Precise Positioning," Proc. of First International Symposium on Precise Positioning with the Global Positioning System, Positioning with GPS, Volume 1, April 15-19, 1985, pp. 37-50.

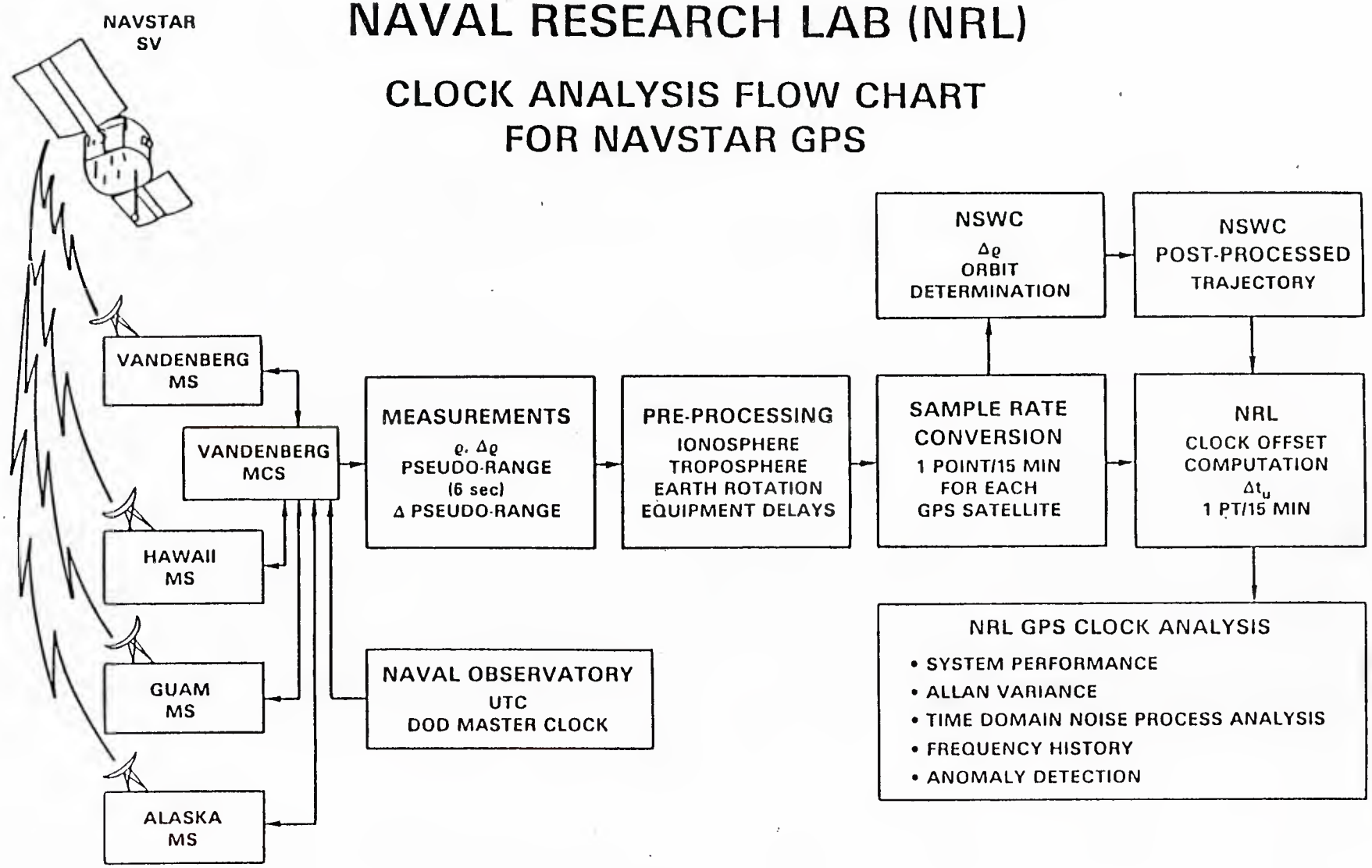
NAVAL RESEARCH LAB (NRL)
CLOCK ANALYSIS FLOW CHART
FOR NAVSTAR GPS
NAVSTAR
SV
VANDENBERG
MS
VANDENBERG
MCS
HAWAII
MS
GUAM
MS
ALASKA
MS
MEASUREMENTS
ϱ, Δϱ
PSEUDO-RANGE
(6 sec)
Δ PSEUDO-RANGE
PRE-PROCESSING
IONOSPHERE
TROPOSPHERE
EARTH ROTATION
EQUIPMENT DELAYS
SAMPLE RATE
CONVERSION
1 POINT/15 MIN
FOR EACH
GPS SATELLITE
NSWC
Δϱ
ORBIT
DETERMINATION
NSWC
POST-PROCESSED
TRAJECTORY
NRL
CLOCK OFFSET
COMPUTATION
Δt_u
1 PT/15 MIN
NAVAL OBSERVATORY
UTC
DOD MASTER CLOCK
NRL GPS CLOCK ANALYSIS
• SYSTEM PERFORMANCE
• ALLAN VARIANCE
• TIME DOMAIN NOISE PROCESS ANALYSIS
• FREQUENCY HISTORY
• ANOMALY DETECTION

Figure 1

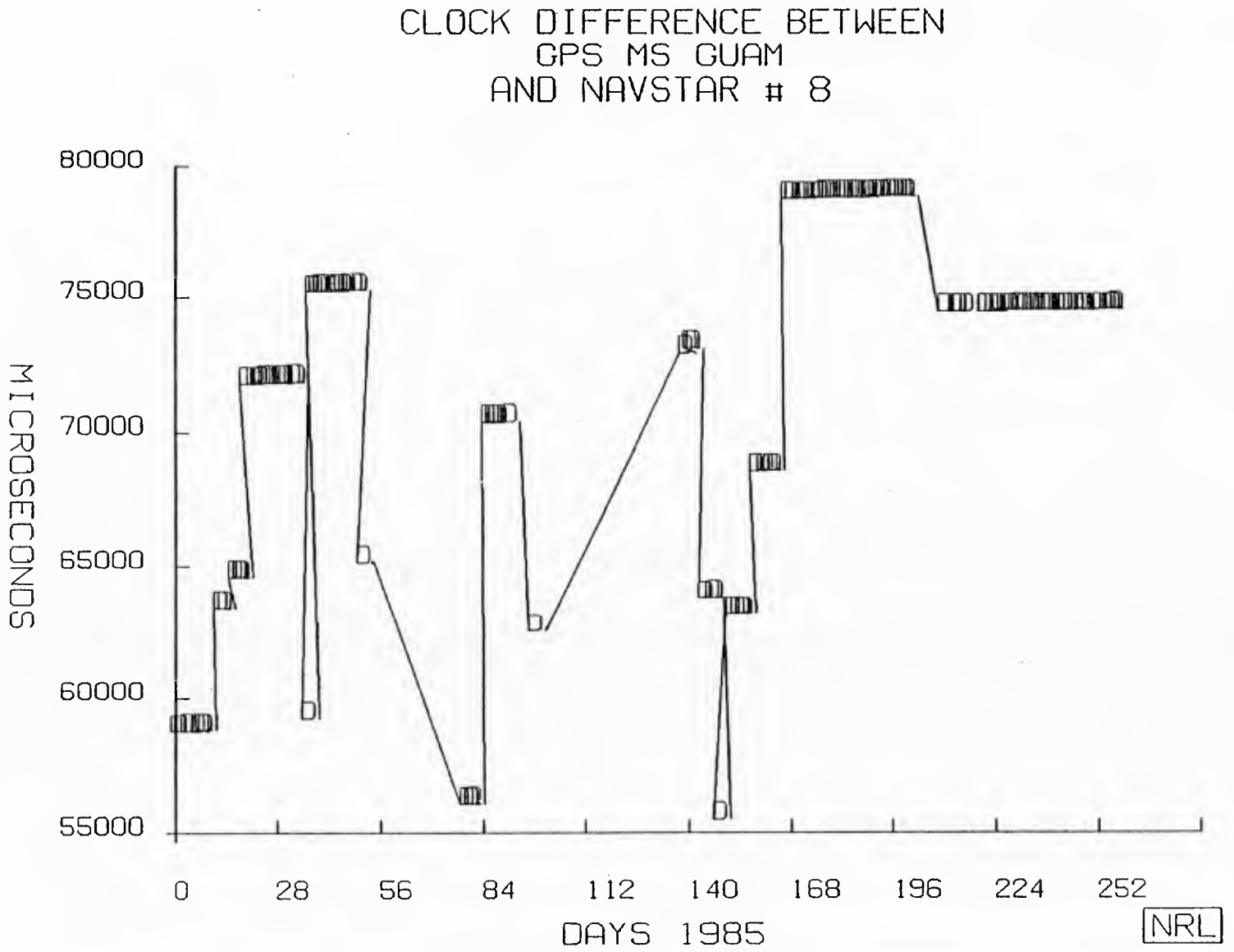
CLOCK DIFFERENCE BETWEEN
GPS MS GUAM
AND NAVSTAR # 8
MICROSECONDS
80000
75000
70000
65000
60000
55000
0
28
56
84
112
140
168
196
224
252
DAYS 1985
NRL

Figure 2

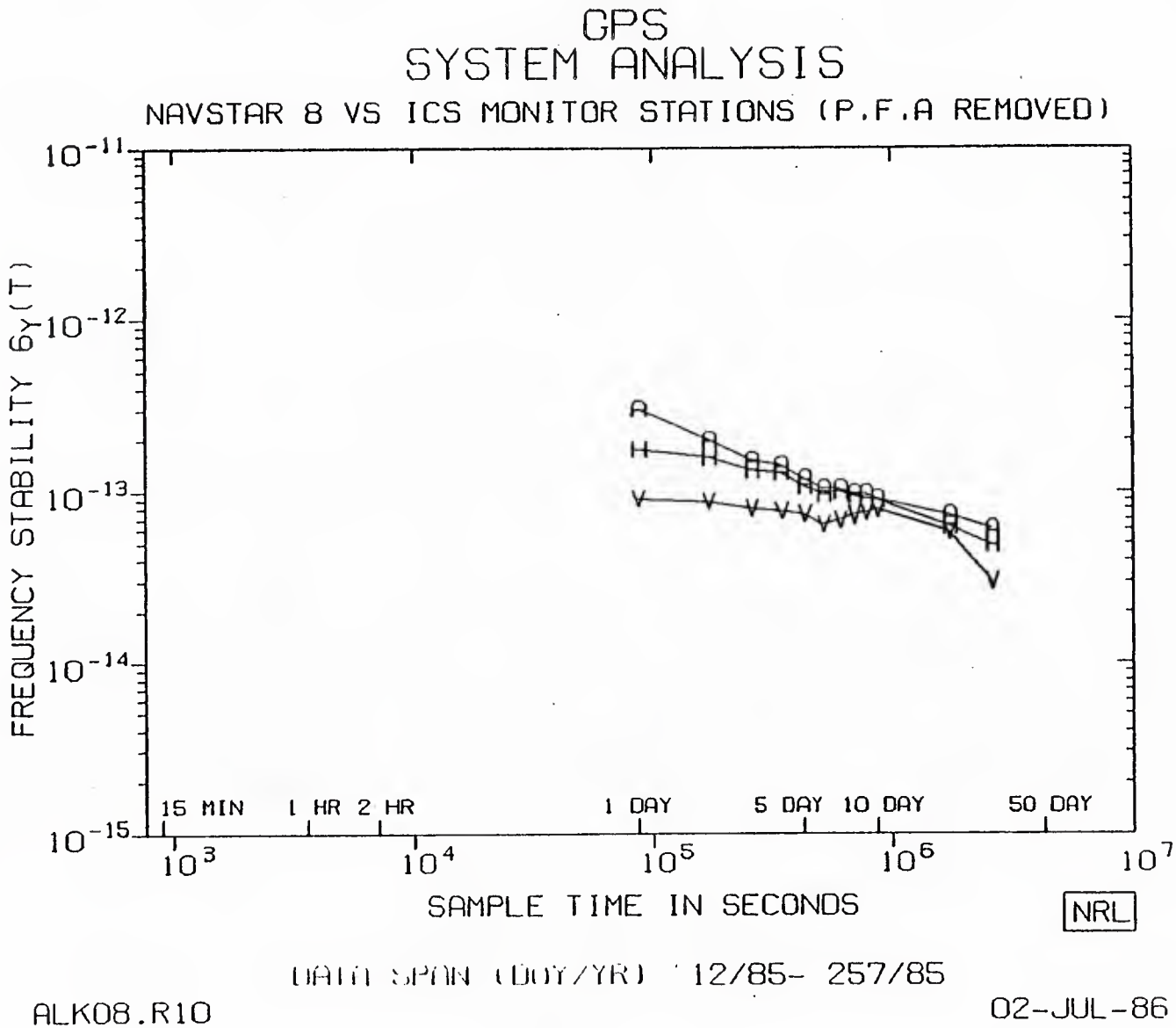
GPS
SYSTEM ANALYSIS
NAVSTAR 8 VS ICS MONITOR STATIONS (P.F.A REMOVED)
FREQUENCY STABILITY σy(T)
10^-11
10^-12
10^-13
10^-14
10^-15
15 MIN
1 HR
2 HR
1 DAY
5 DAY
10 DAY
50 DAY
10^3
10^4
10^5
10^6
10^7
SAMPLE TIME IN SECONDS
NRL
DATA SPAN (DOY/YR) 12/85- 257/85
ALK08.R10
02-JUL-86

Figure 3

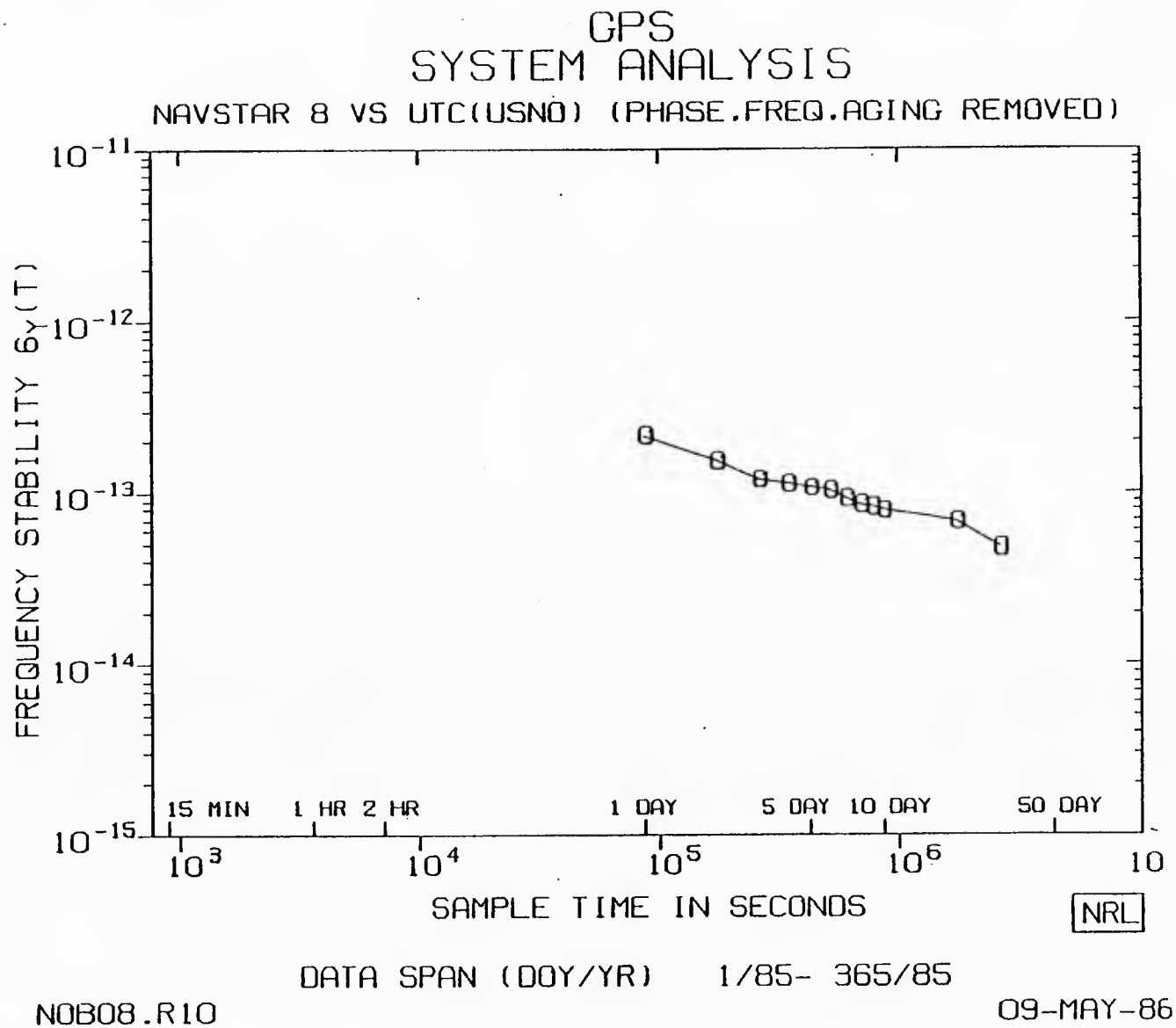
GPS
SYSTEM ANALYSIS
NAVSTAR 8 VS UTC(USNO) (PHASE.FREQ.AGING REMOVED)
FREQUENCY STABILITY σy(T)
10^-11
10^-12
10^-13
10^-14
10^-15
15 MIN
1 HR
2 HR
1 DAY
5 DAY
10 DAY
50 DAY
10^3
10^4
10^5
10^6
10
SAMPLE TIME IN SECONDS
NRL
DATA SPAN (DOY/YR) 1/85- 365/85
NOB08.R10
09-MAY-86

Figure 4

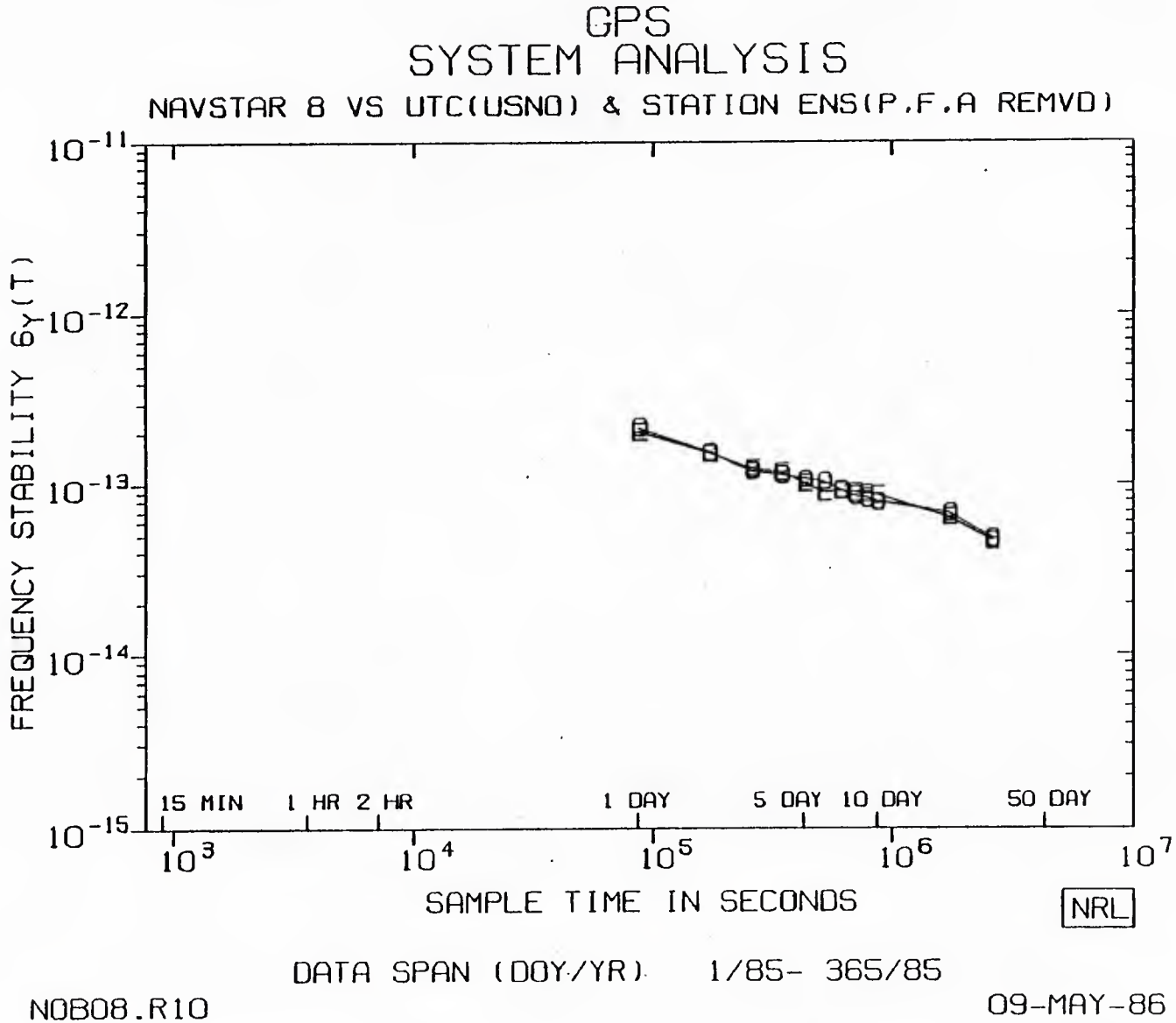
GPS
SYSTEM ANALYSIS
NAVSTAR 8 VS UTC(USNO) & STATION ENS(P.F.A REMVD)
FREQUENCY STABILITY $\sigma_y(T)$
10^{-11}
10^{-12}
10^{-13}
10^{-14}
10^{-15}
15 MIN
1 HR
2 HR
1 DAY
5 DAY
10 DAY
50 DAY
10^3
10^4
10^5
10^6
10^7
SAMPLE TIME IN SECONDS
NRL
DATA SPAN (DOY/YR) 1/85- 365/85
NOB08.R10
09-MAY-86

Figure 5

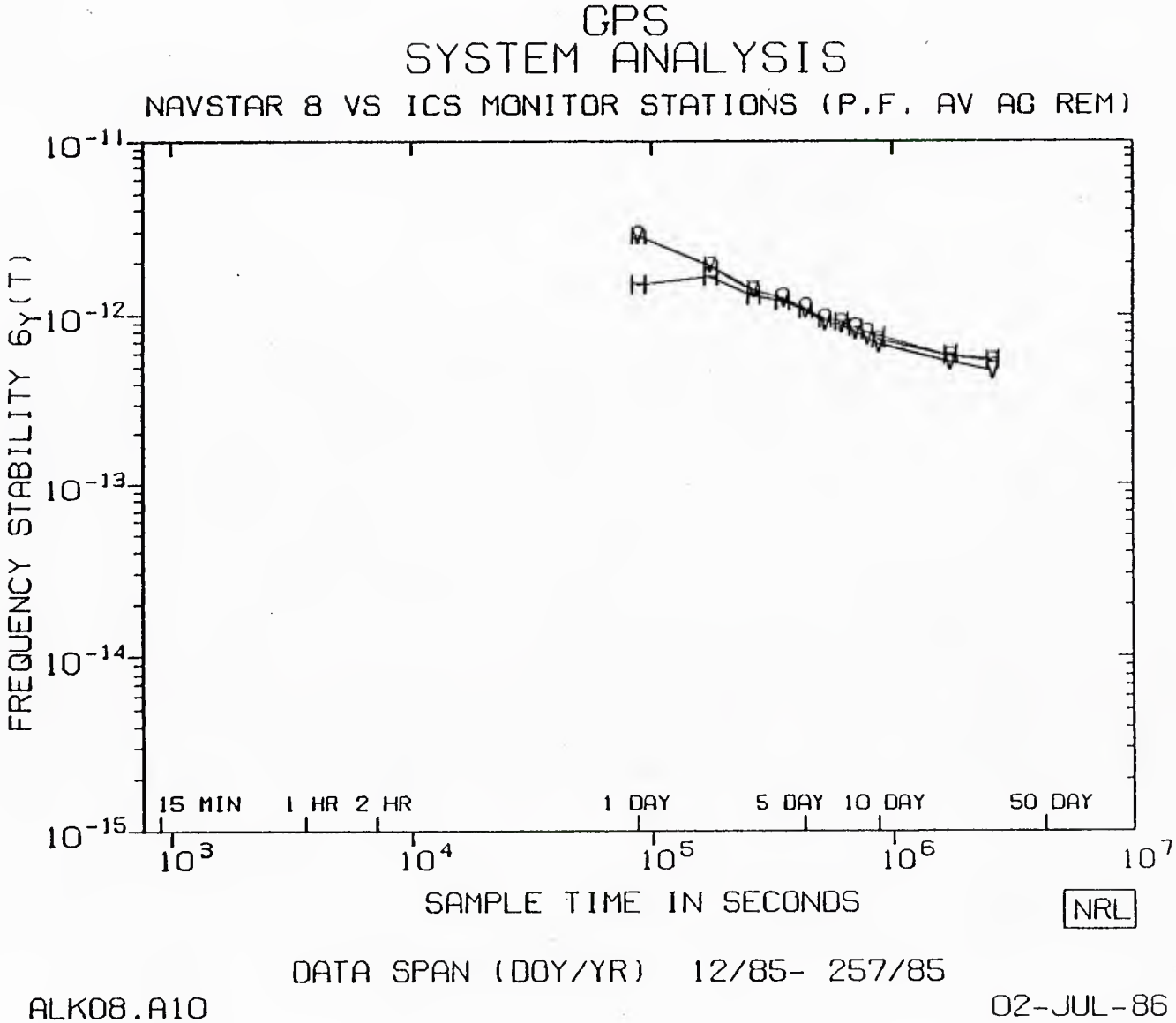
GPS
SYSTEM ANALYSIS
NAVSTAR 8 VS ICS MONITOR STATIONS (P.F. AV AG REM)
FREQUENCY STABILITY $6_y(T)$
10^{-11}
10^{-12}
10^{-13}
10^{-14}
10^{-15}
15 MIN
1 HR
2 HR
1 DAY
5 DAY
10 DAY
50 DAY
10^3
10^4
10^5
10^6
10^7
SAMPLE TIME IN SECONDS
NRL
DATA SPAN (DOY/YR) 12/85- 257/85
ALK08.A10
02-JUL-86

Figure 6

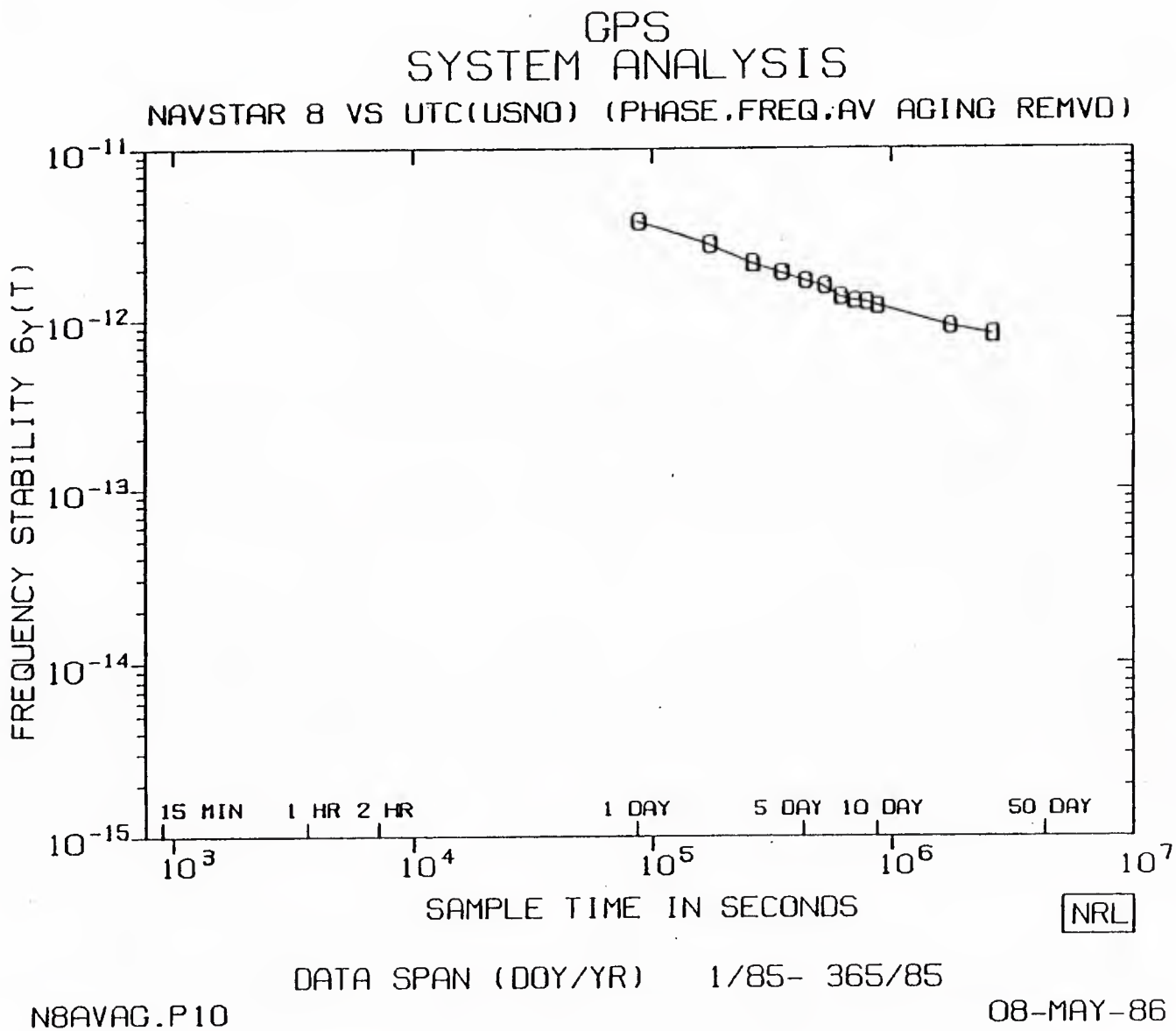
GPS
SYSTEM ANALYSIS
NAVSTAR 8 VS UTC(USNO) (PHASE,FREQ,AV AGING REMVD)
FREQUENCY STABILITY σy(T)
10^-11
10^-12
10^-13
10^-14
10^-15
15 MIN
1 HR
2 HR
1 DAY
5 DAY
10 DAY
50 DAY
10^3
10^4
10^5
10^6
10^7
SAMPLE TIME IN SECONDS
NRL
DATA SPAN (DOY/YR) 1/85- 365/85
N8AVAG.P10
08-MAY-86

Figure 7

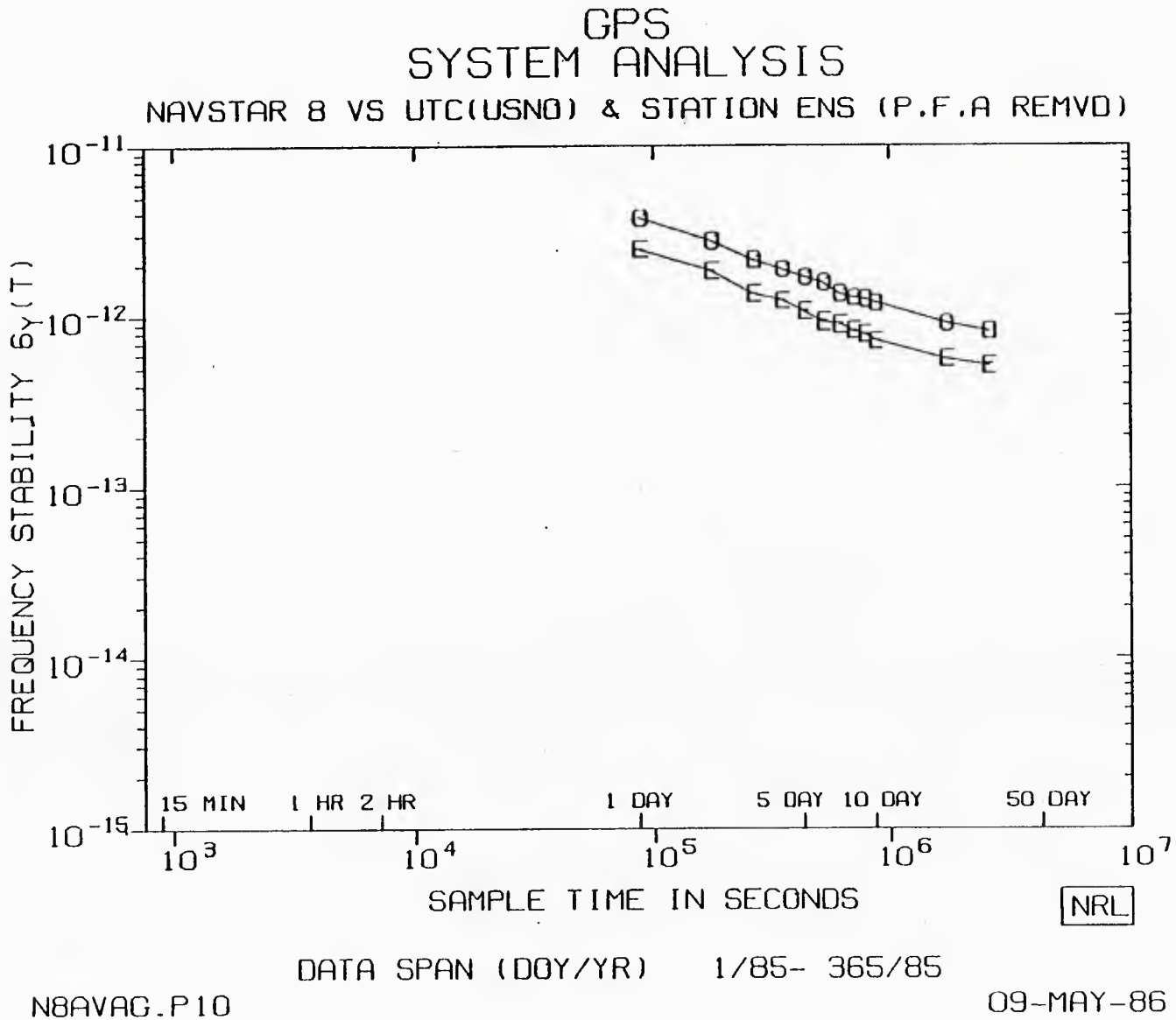
GPS
SYSTEM ANALYSIS
NAVSTAR 8 VS UTC(USNO) & STATION ENS (P.F.A REMVD)
FREQUENCY STABILITY $\sigma_y(T)$
10^{-11}
10^{-12}
10^{-13}
10^{-14}
10^{-15}
15 MIN
1 HR
2 HR
1 DAY
5 DAY
10 DAY
50 DAY
10^3
10^4
10^5
10^6
10^7
SAMPLE TIME IN SECONDS
NRL
DATA SPAN (DOY/YR) 1/85- 365/85
N8AVAC.P10
09-MAY-86

Figure 8

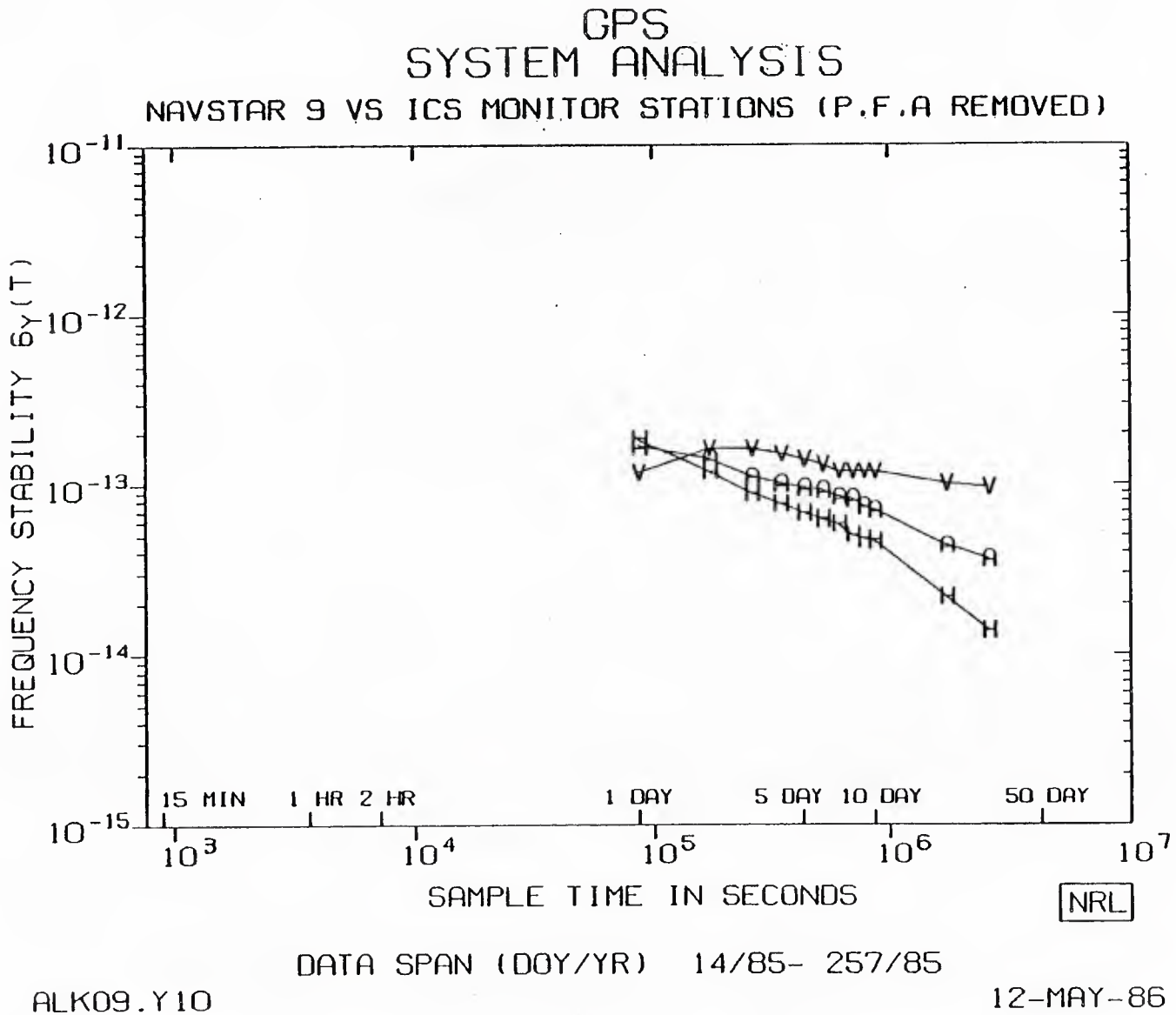
GPS
SYSTEM ANALYSIS
NAVSTAR 9 VS ICS MONITOR STATIONS (P.F.A REMOVED)
FREQUENCY STABILITY $\sigma_y(T)$
10^{-11}
10^{-12}
10^{-13}
10^{-14}
10^{-15}
15 MIN
1 HR
2 HR
1 DAY
5 DAY
10 DAY
50 DAY
10^3
10^4
10^5
10^6
10^7
SAMPLE TIME IN SECONDS
NRL
DATA SPAN (DOY/YR) 14/85- 257/85
ALK09.Y10
12-MAY-86

Figure 9

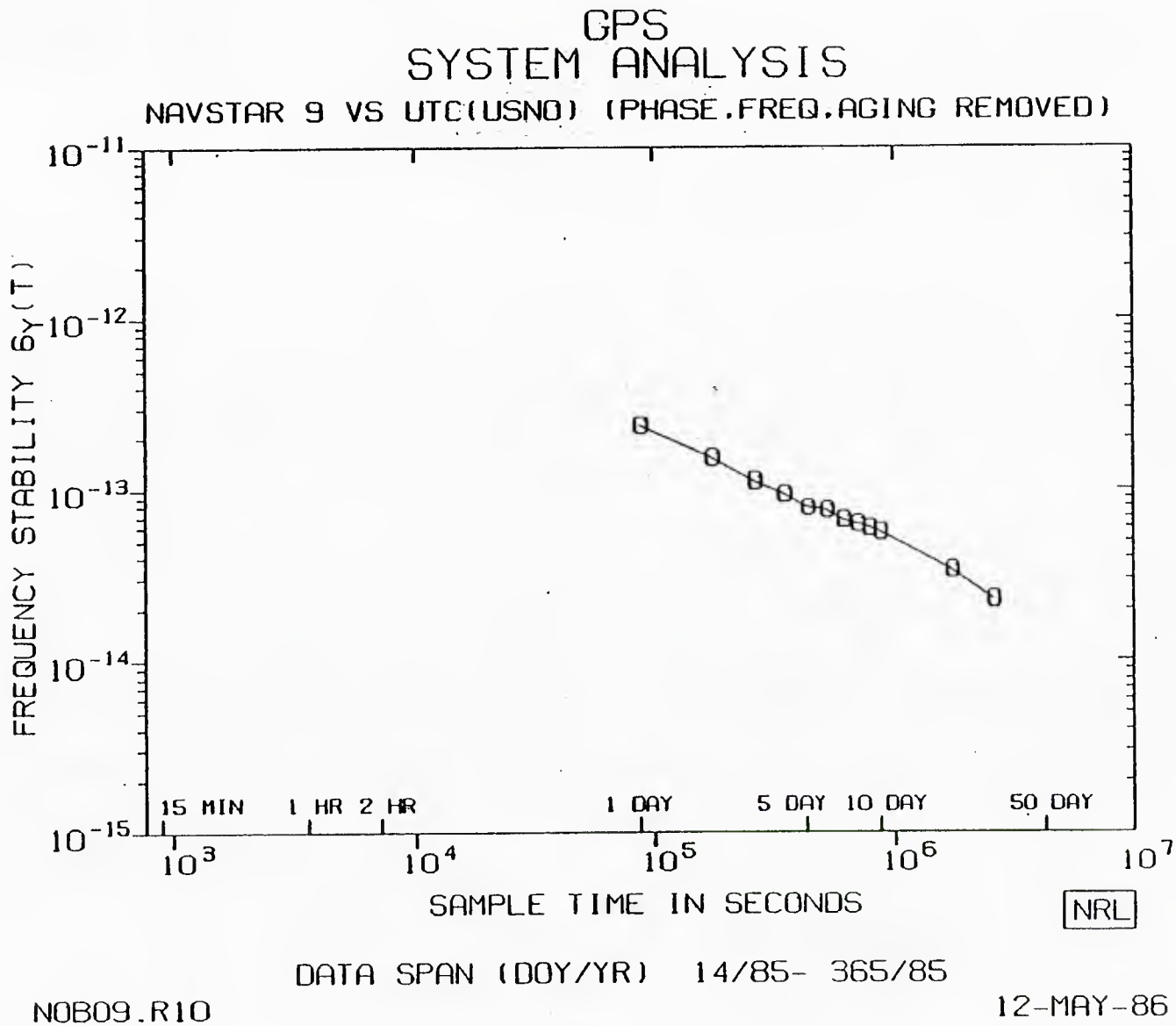
GPS
SYSTEM ANALYSIS
NAVSTAR 9 VS UTC(USNO) (PHASE,FREQ,AGING REMOVED)
FREQUENCY STABILITY σy(T)
10^-11
10^-12
10^-13
10^-14
10^-15
15 MIN
1 HR
2 HR
1 DAY
5 DAY
10 DAY
50 DAY
10^3
10^4
10^5
10^6
10^7
SAMPLE TIME IN SECONDS
NRL
DATA SPAN (DOY/YR) 14/85- 365/85
NOB09.R10
12-MAY-86

Figure 10

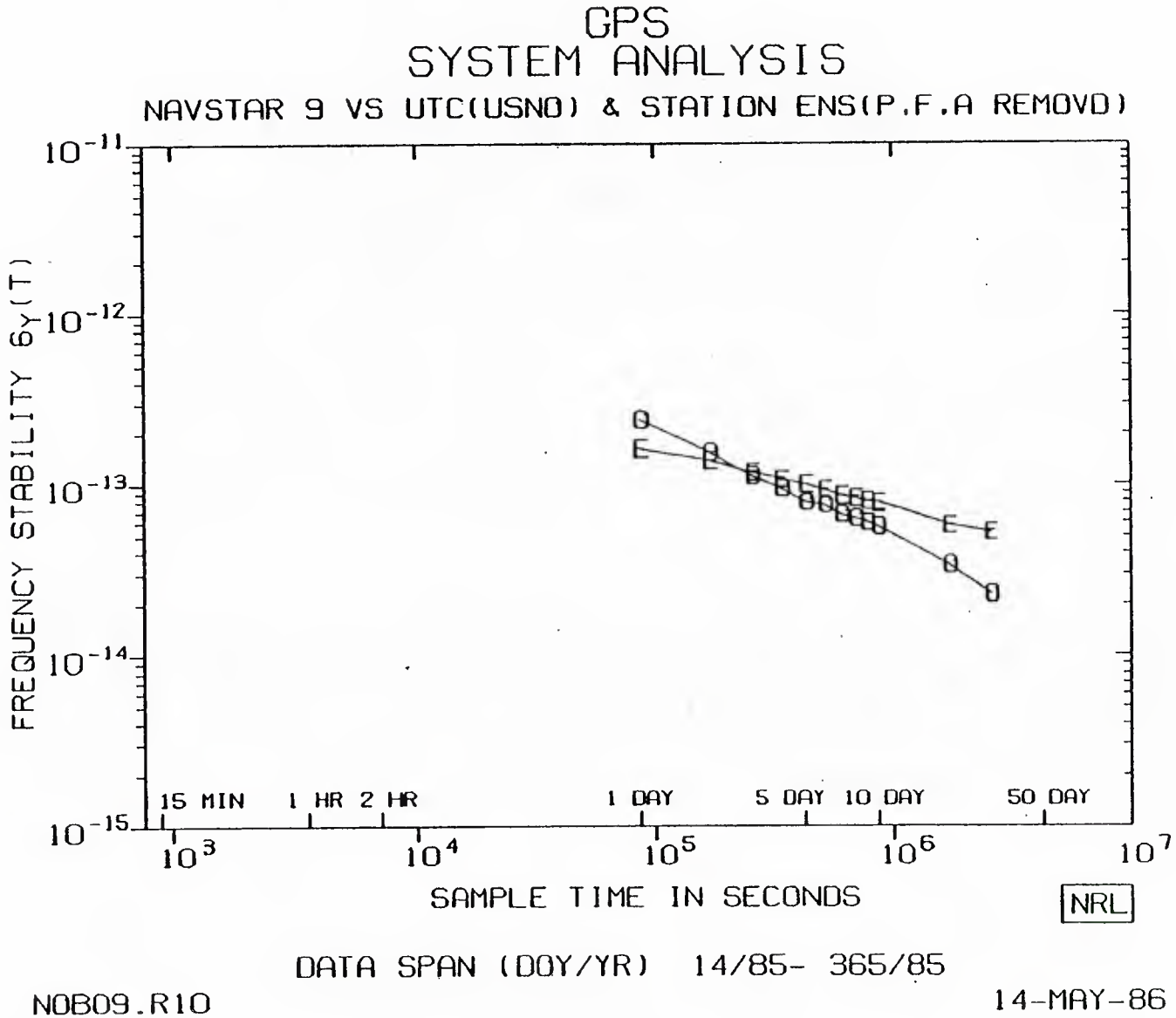
GPS
SYSTEM ANALYSIS
NAVSTAR 9 VS UTC(USNO) & STATION ENS(P,F,A REMOVD)
FREQUENCY STABILITY σy(T)
10^-11
10^-12
10^-13
10^-14
10^-15
15 MIN
1 HR
2 HR
1 DAY
5 DAY
10 DAY
50 DAY
10^3
10^4
10^5
10^6
10^7
SAMPLE TIME IN SECONDS
NRL
DATA SPAN (DOY/YR) 14/85- 365/85
NOB09.R10
14-MAY-86

Figure 11

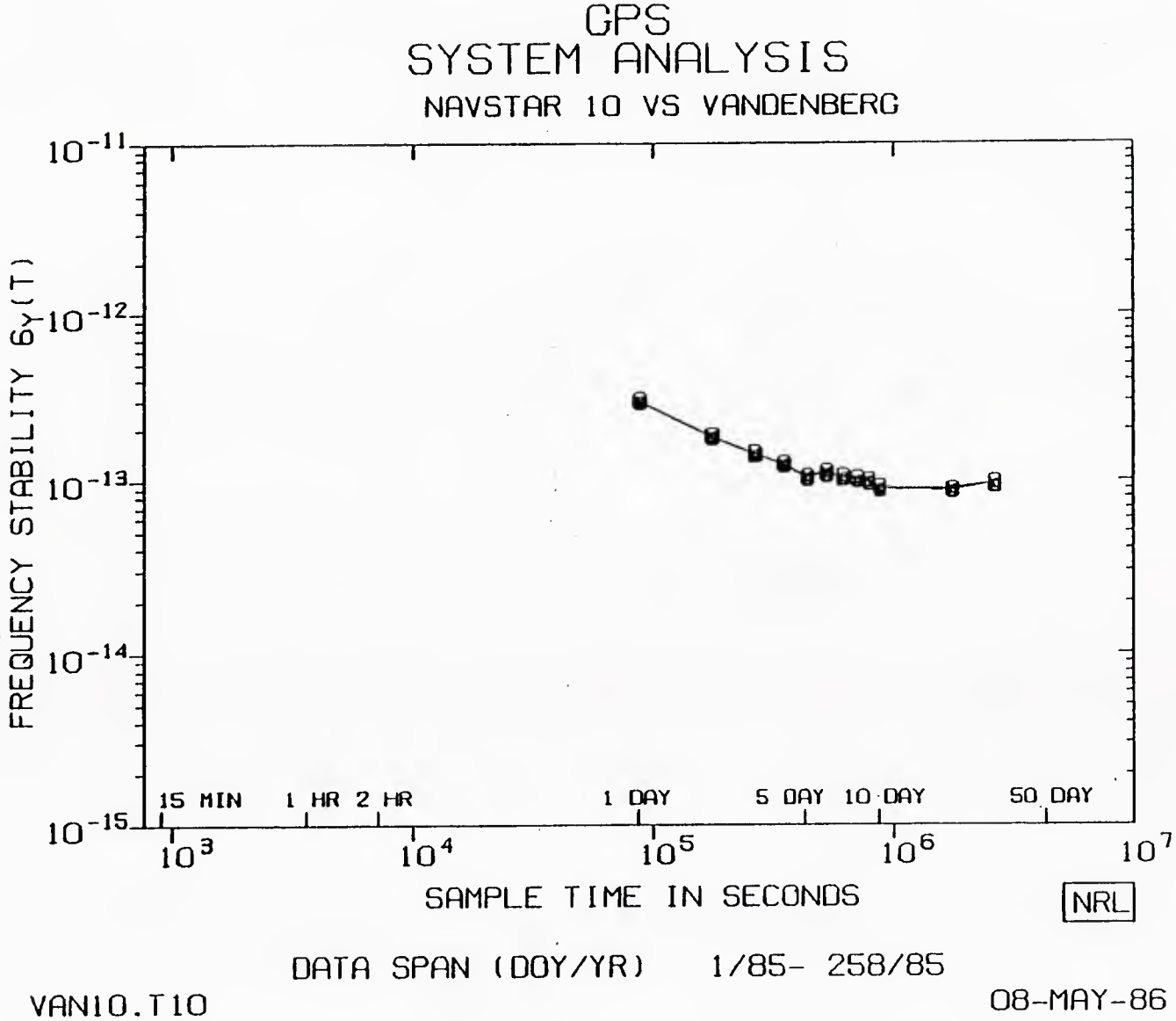
GPS
SYSTEM ANALYSIS
NAVSTAR 10 VS VANDENBERG
FREQUENCY STABILITY $\sigma_y(T)$
10^{-11}
10^{-12}
10^{-13}
10^{-14}
10^{-15}
15 MIN
1 HR
2 HR
1 DAY
5 DAY
10 DAY
50 DAY
10^3
10^4
10^5
10^6
10^7
SAMPLE TIME IN SECONDS
NRL
DATA SPAN (DOY/YR) 1/85- 258/85
VAN10.T10
08-MAY-86

Figure 12

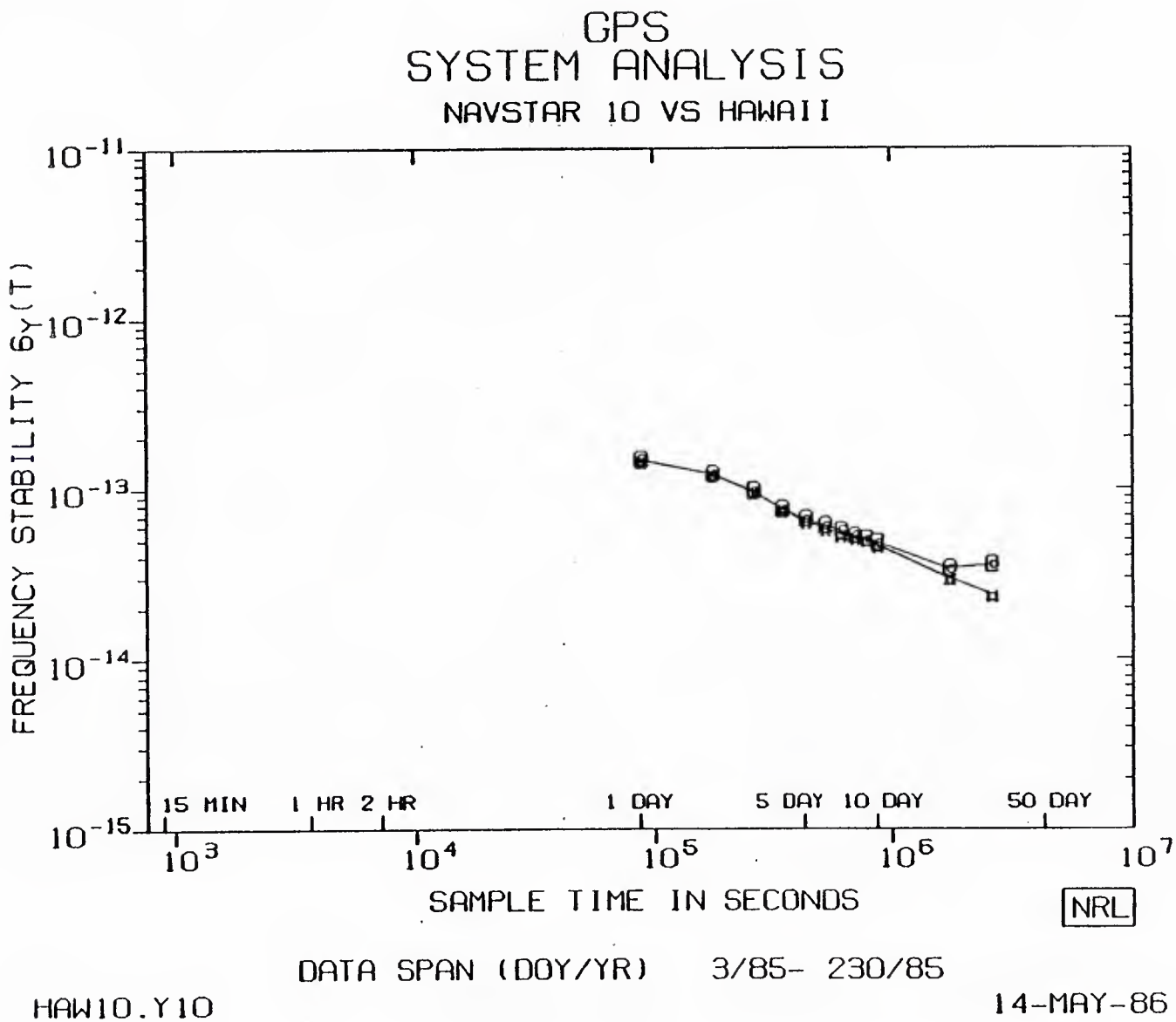
GPS
SYSTEM ANALYSIS
NAVSTAR 10 VS HAWAII
FREQUENCY STABILITY $6_Y(T)$
10^{-11}
10^{-12}
10^{-13}
10^{-14}
10^{-15}
15 MIN
1 HR
2 HR
1 DAY
5 DAY
10 DAY
50 DAY
10^3
10^4
10^5
10^6
10^7
SAMPLE TIME IN SECONDS
NRL
DATA SPAN (DOY/YR) 3/85- 230/85
HAW10.Y10
14-MAY-86

Figure 13

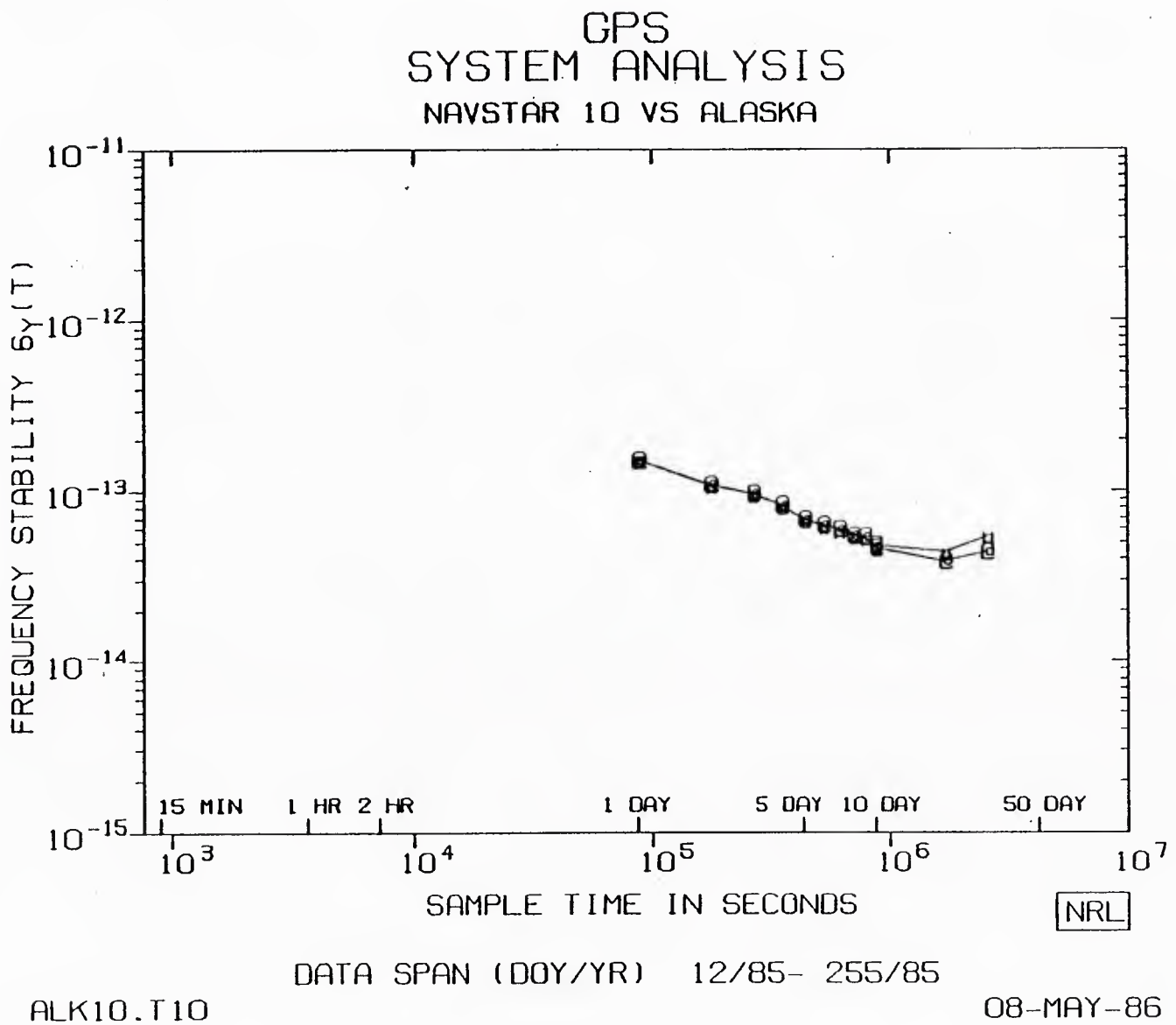
GPS
SYSTEM ANALYSIS
NAVSTAR 10 VS ALASKA
FREQUENCY STABILITY σy(T)
10^-11
10^-12
10^-13
10^-14
10^-15
15 MIN
1 HR
2 HR
1 DAY
5 DAY
10 DAY
50 DAY
10^3
10^4
10^5
10^6
10^7
SAMPLE TIME IN SECONDS
NRL
DATA SPAN (DOY/YR) 12/85- 255/85
ALK10.T10
08-MAY-86

Figure 14

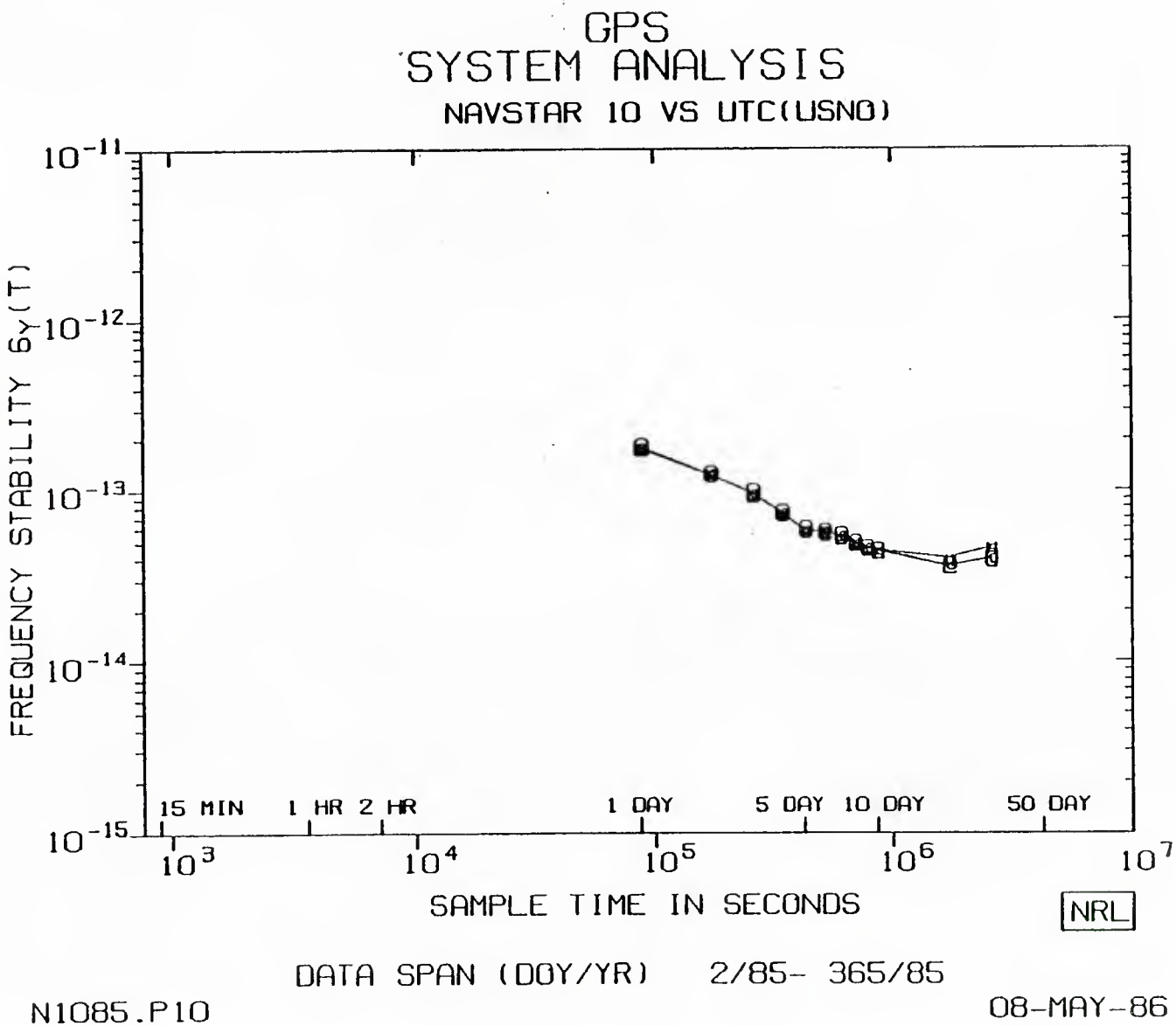
GPS
SYSTEM ANALYSIS
NAVSTAR 10 VS UTC(USNO)
FREQUENCY STABILITY σy(T)
10^-11
10^-12
10^-13
10^-14
10^-15
15 MIN
1 HR
2 HR
1 DAY
5 DAY
10 DAY
50 DAY
10^3
10^4
10^5
10^6
10^7
SAMPLE TIME IN SECONDS
NRL
DATA SPAN (DOY/YR) 2/85- 365/85
N1085.P10
08-MAY-86

Figure 15

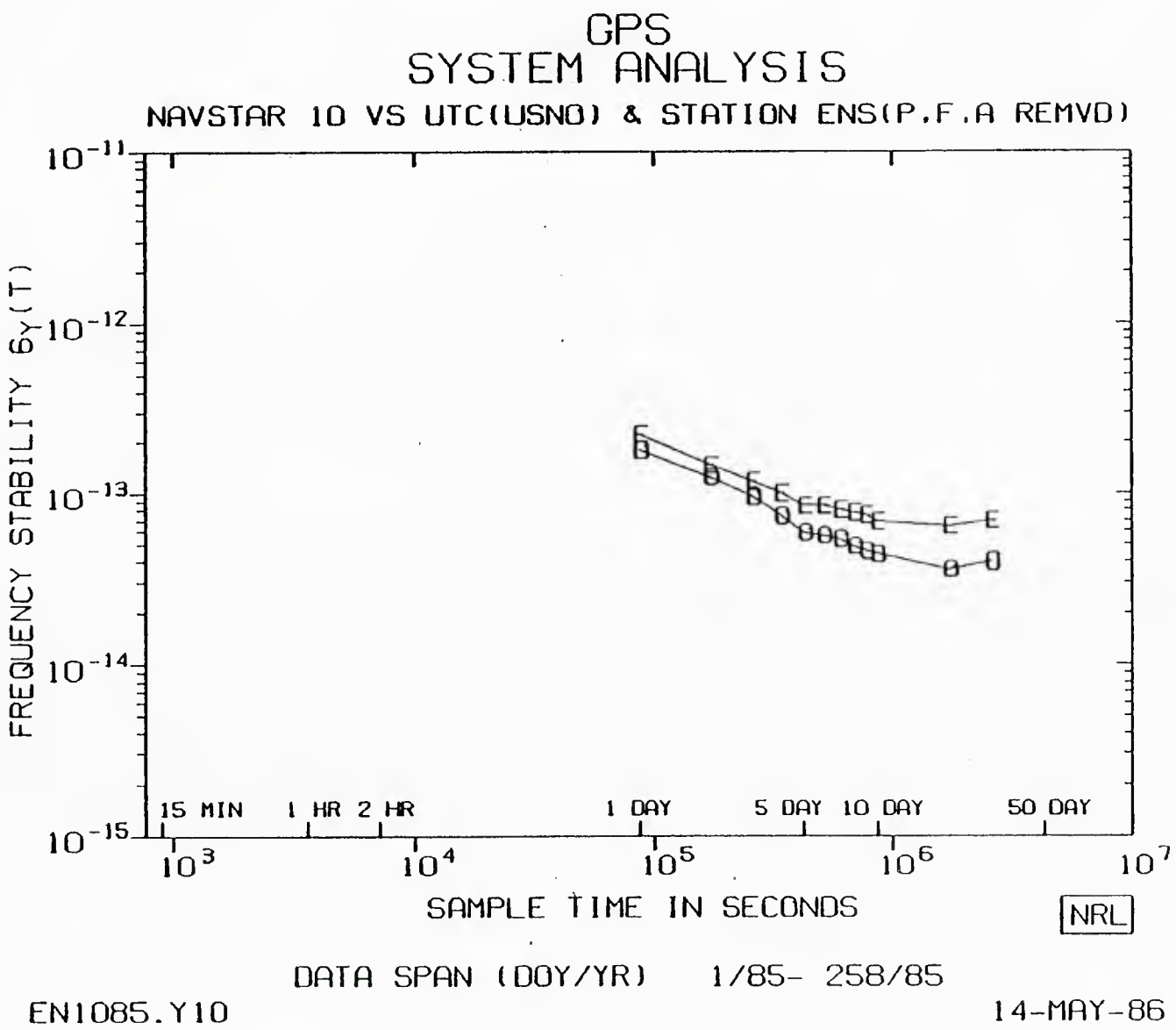
GPS
SYSTEM ANALYSIS
NAVSTAR 10 VS UTC(USNO) & STATION ENS(P,F,A REMVD)
FREQUENCY STABILITY σy(T)
10^-11
10^-12
10^-13
10^-14
10^-15
15 MIN
1 HR
2 HR
1 DAY
5 DAY
10 DAY
50 DAY
10^3
10^4
10^5
10^6
10^7
SAMPLE TIME IN SECONDS
NRL
DATA SPAN (DOY/YR) 1/85- 258/85
EN1085.Y10
14-MAY-86

Figure 16

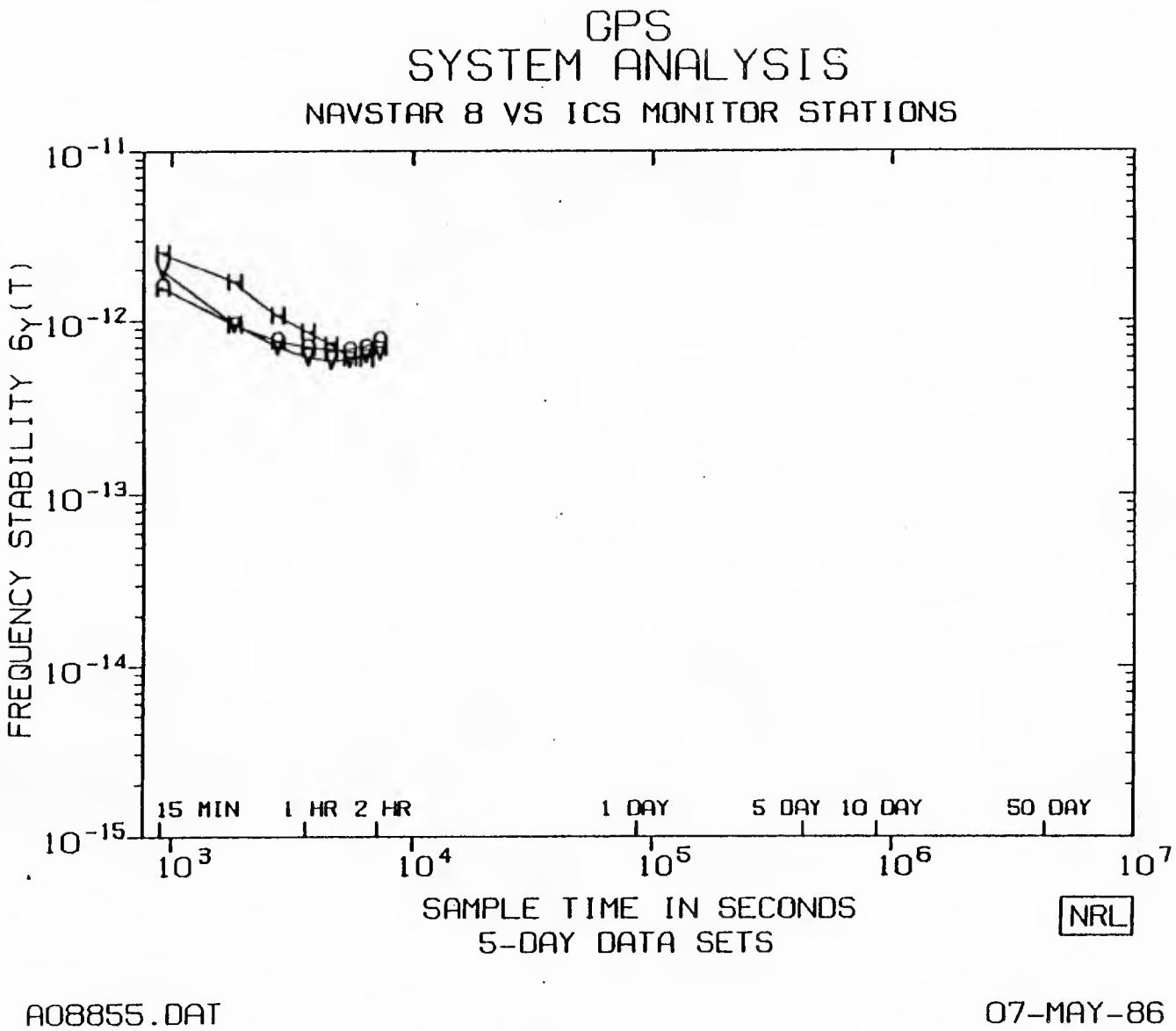
GPS
SYSTEM ANALYSIS
NAVSTAR 8 VS ICS MONITOR STATIONS
FREQUENCY STABILITY σy(T)
10^-11
10^-12
10^-13
10^-14
10^-15
15 MIN
1 HR
2 HR
1 DAY
5 DAY
10 DAY
50 DAY
10^3
10^4
10^5
10^6
10^7
SAMPLE TIME IN SECONDS
5-DAY DATA SETS
NRL
A08855.DAT
07-MAY-86

Figure 17

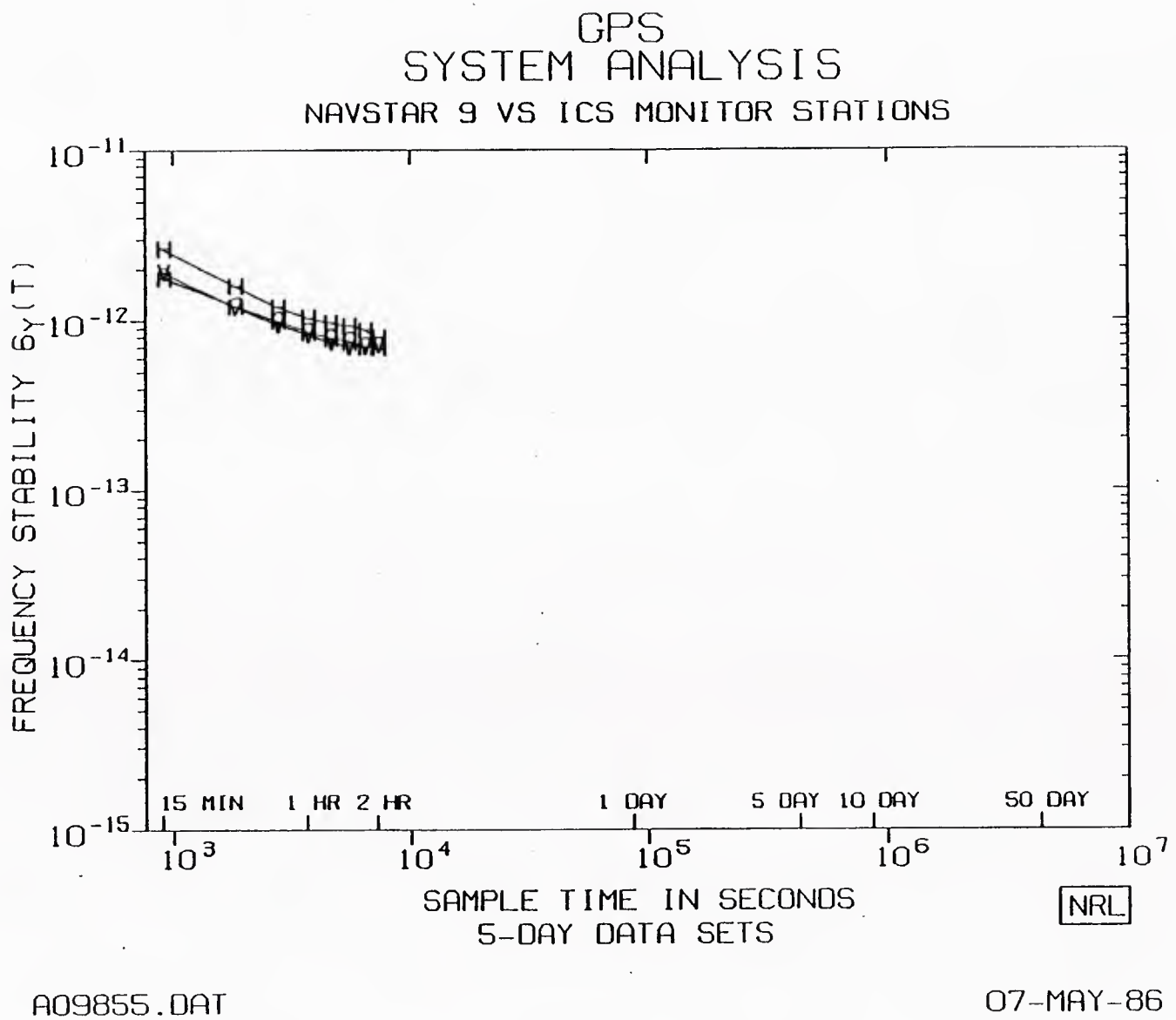
GPS
SYSTEM ANALYSIS
NAVSTAR 9 VS ICS MONITOR STATIONS
FREQUENCY STABILITY σy(T)
10^-11
10^-12
10^-13
10^-14
10^-15
15 MIN
1 HR
2 HR
1 DAY
5 DAY
10 DAY
50 DAY
10^3
10^4
10^5
10^6
10^7
SAMPLE TIME IN SECONDS
5-DAY DATA SETS
NRL
A09855.DAT
07-MAY-86

Figure 18

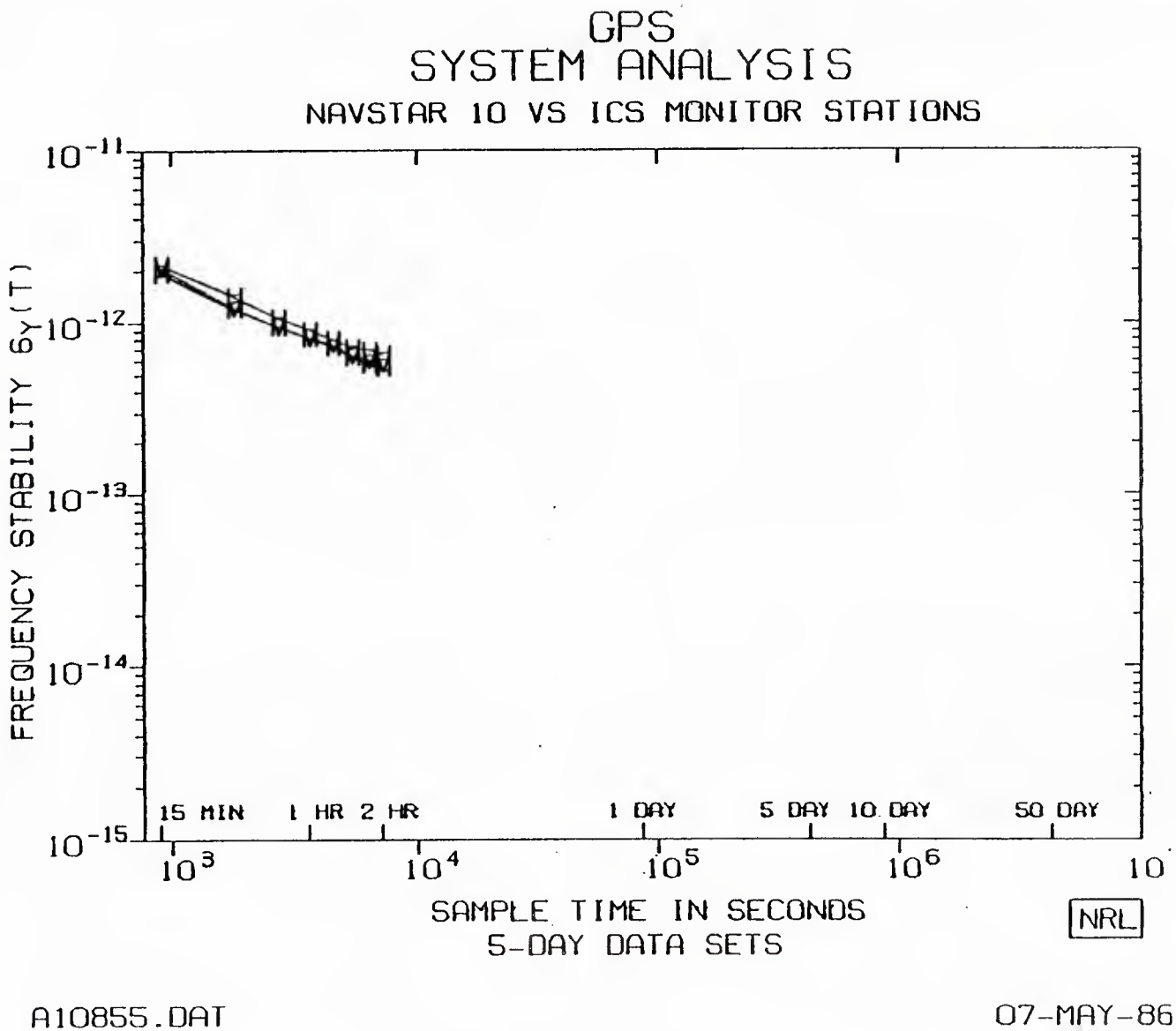
GPS
SYSTEM ANALYSIS
NAVSTAR 10 VS ICS MONITOR STATIONS
FREQUENCY STABILITY σy(T)
10^-11
10^-12
10^-13
10^-14
10^-15
15 MIN
1 HR
2 HR
1 DAY
5 DAY
10 DAY
50 DAY
10^3
10^4
10^5
10^6
10
SAMPLE TIME IN SECONDS
5-DAY DATA SETS
NRL
A10855.DAT
07-MAY-86

Figure 19

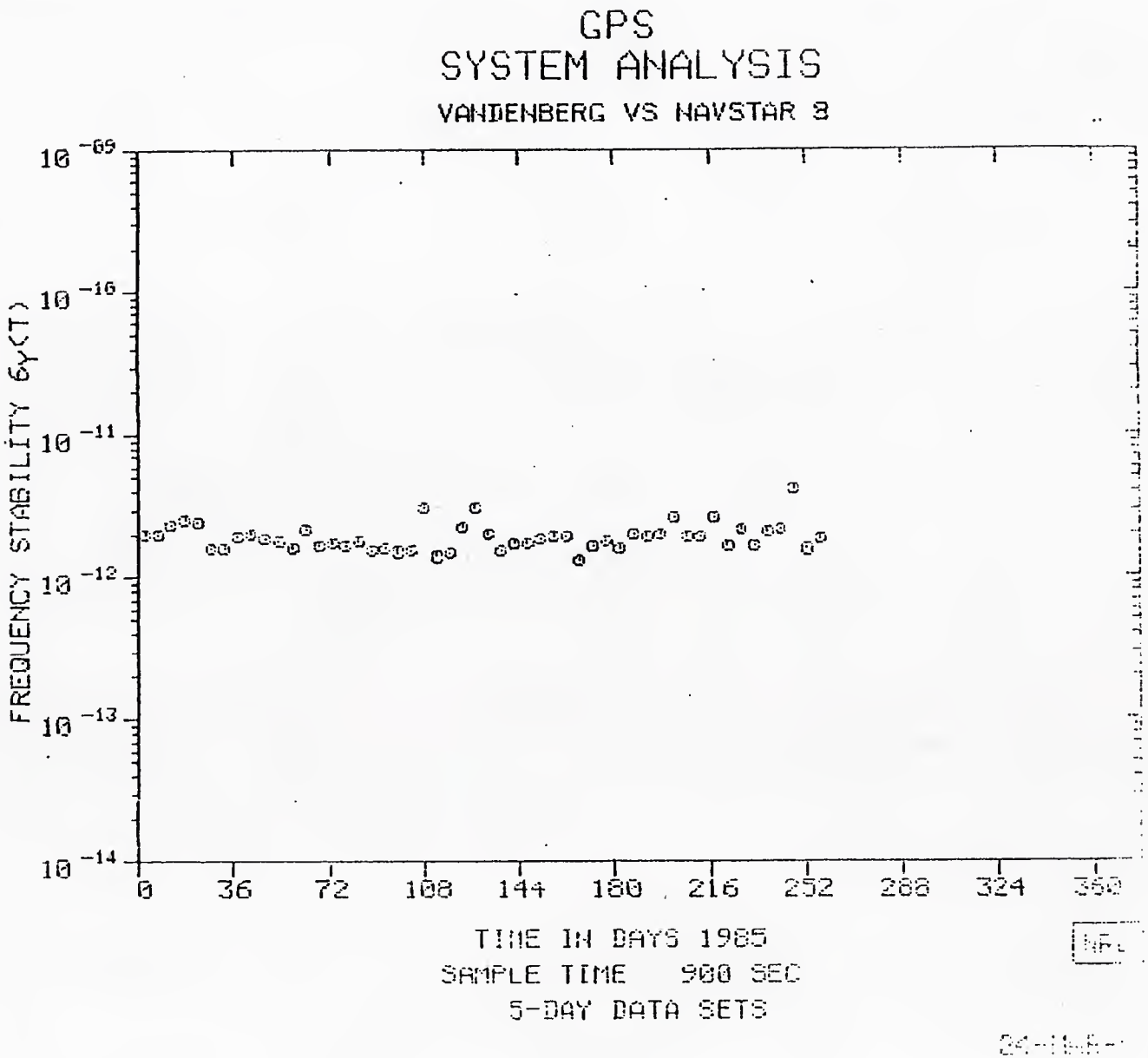
GPS
SYSTEM ANALYSIS
VANDENBERG VS NAVSTAR 8
FREQUENCY STABILITY σy(T)
10 -09
10 -10
10 -11
10 -12
10 -13
10 -14
0
36
72
108
144
180
216
252
288
324
360
TIME IN DAYS 1985
SAMPLE TIME 900 SEC
5-DAY DATA SETS

Figure 20

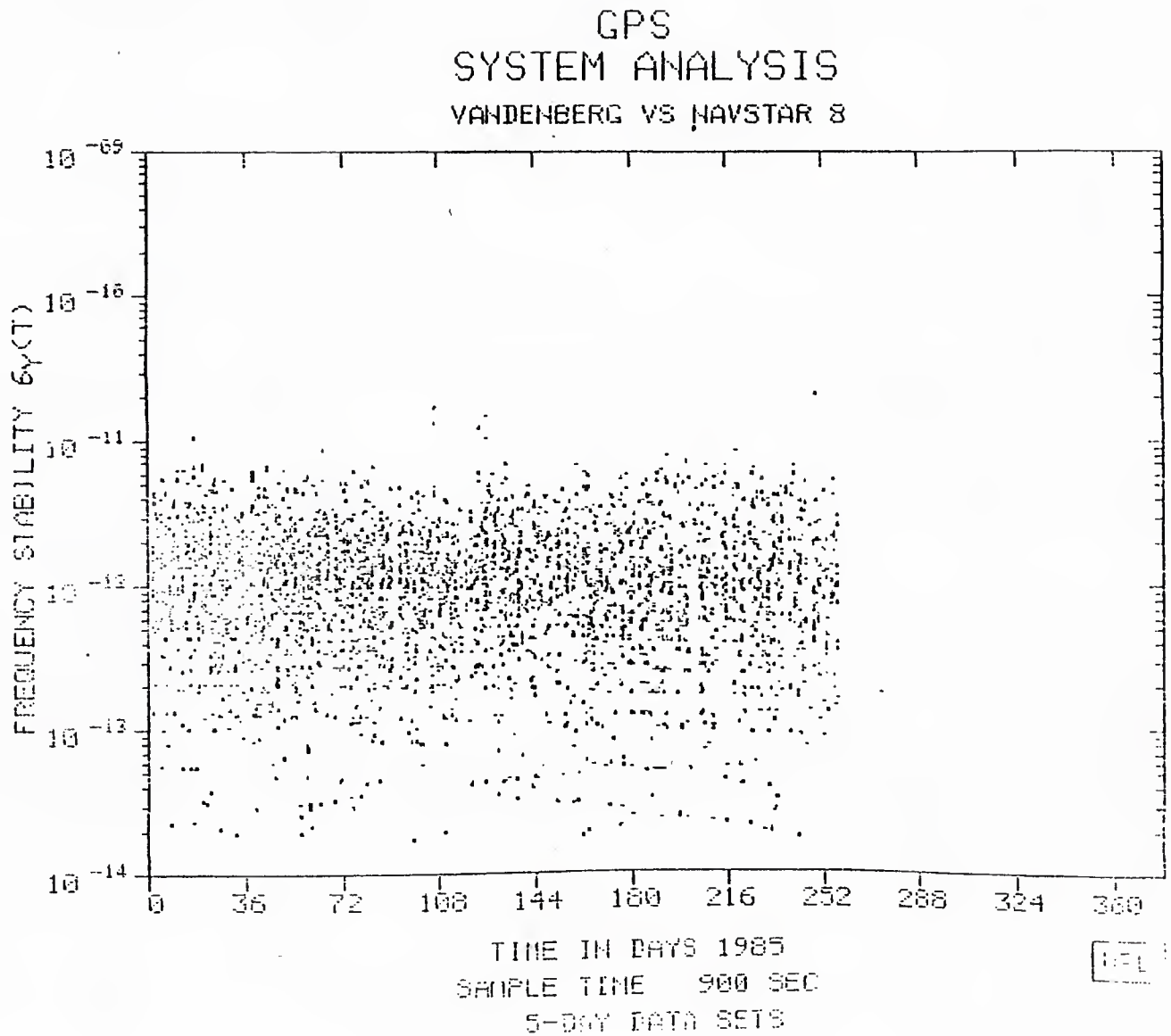
GPS
SYSTEM ANALYSIS
VANDENBERG VS NAVSTAR 8
FREQUENCY STABILITY 6y(T)
10 -09
10 -10
10 -11
10 -12
10 -13
10 -14
0
36
72
108
144
180
216
252
288
324
360
TIME IN DAYS 1985
SAMPLE TIME 900 SEC
5-DAY DATA SETS

Figure 21

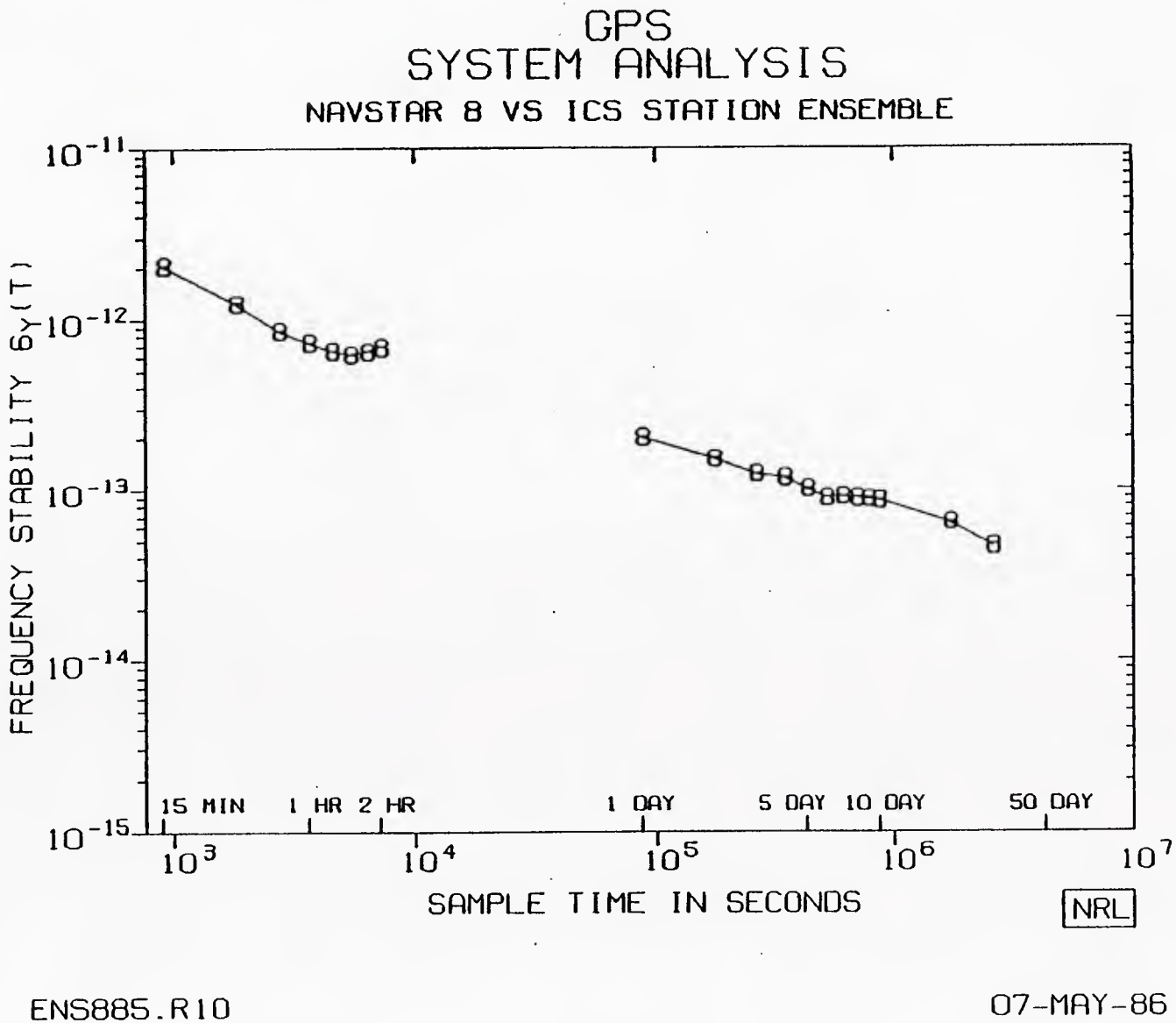
GPS
SYSTEM ANALYSIS
NAVSTAR 8 VS ICS STATION ENSEMBLE
FREQUENCY STABILITY σy(T)
10^-11
10^-12
10^-13
10^-14
10^-15
15 MIN
1 HR
2 HR
1 DAY
5 DAY
10 DAY
50 DAY
10^3
10^4
10^5
10^6
10^7
SAMPLE TIME IN SECONDS
NRL
ENS885.R10
07-MAY-86

Figure 22

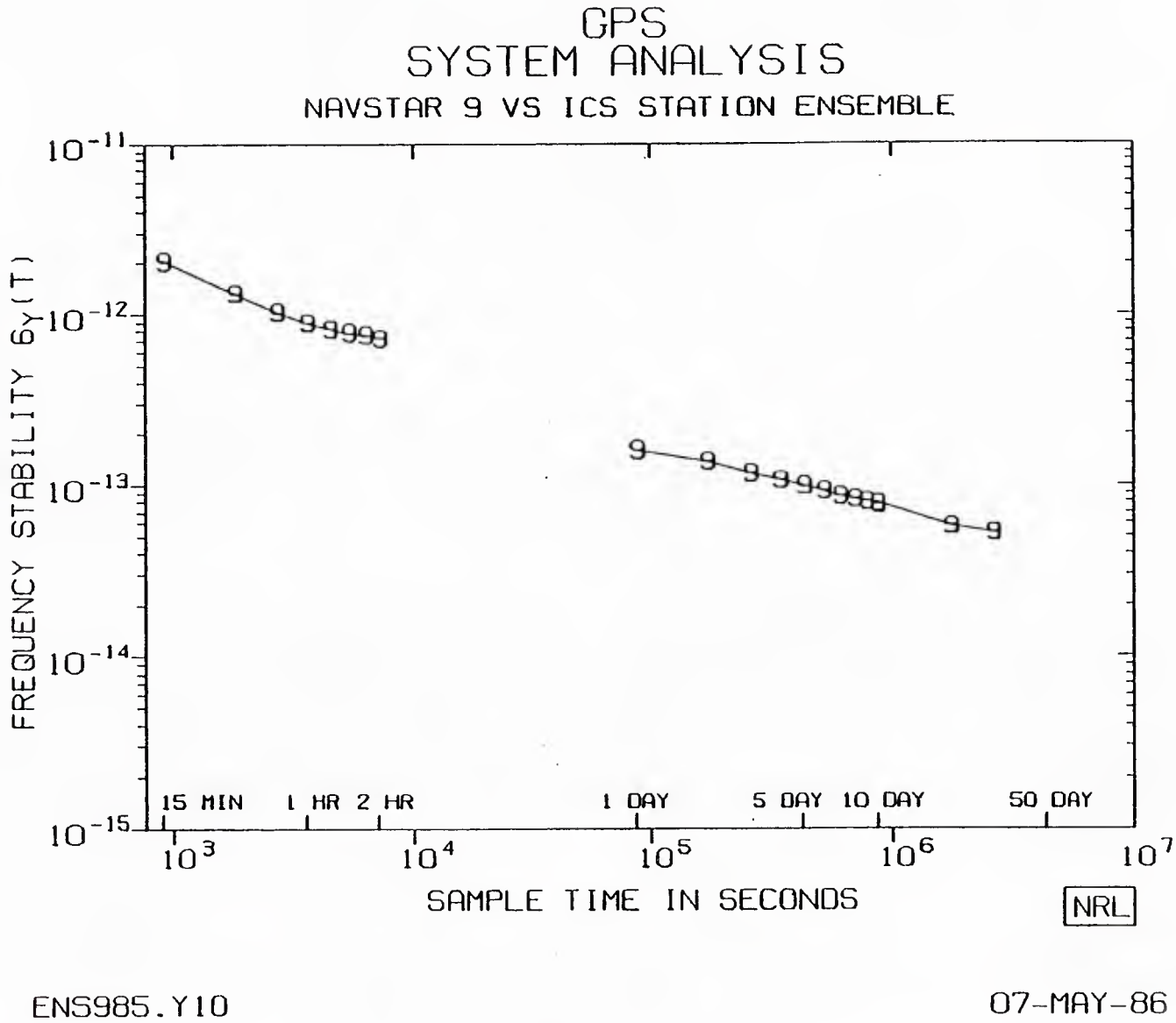
GPS
SYSTEM ANALYSIS
NAVSTAR 9 VS ICS STATION ENSEMBLE
FREQUENCY STABILITY σy(T)
10^-11
10^-12
10^-13
10^-14
10^-15
15 MIN
1 HR
2 HR
1 DAY
5 DAY
10 DAY
50 DAY
10^3
10^4
10^5
10^6
10^7
SAMPLE TIME IN SECONDS
NRL
ENS985.Y10
07-MAY-86

Figure 23

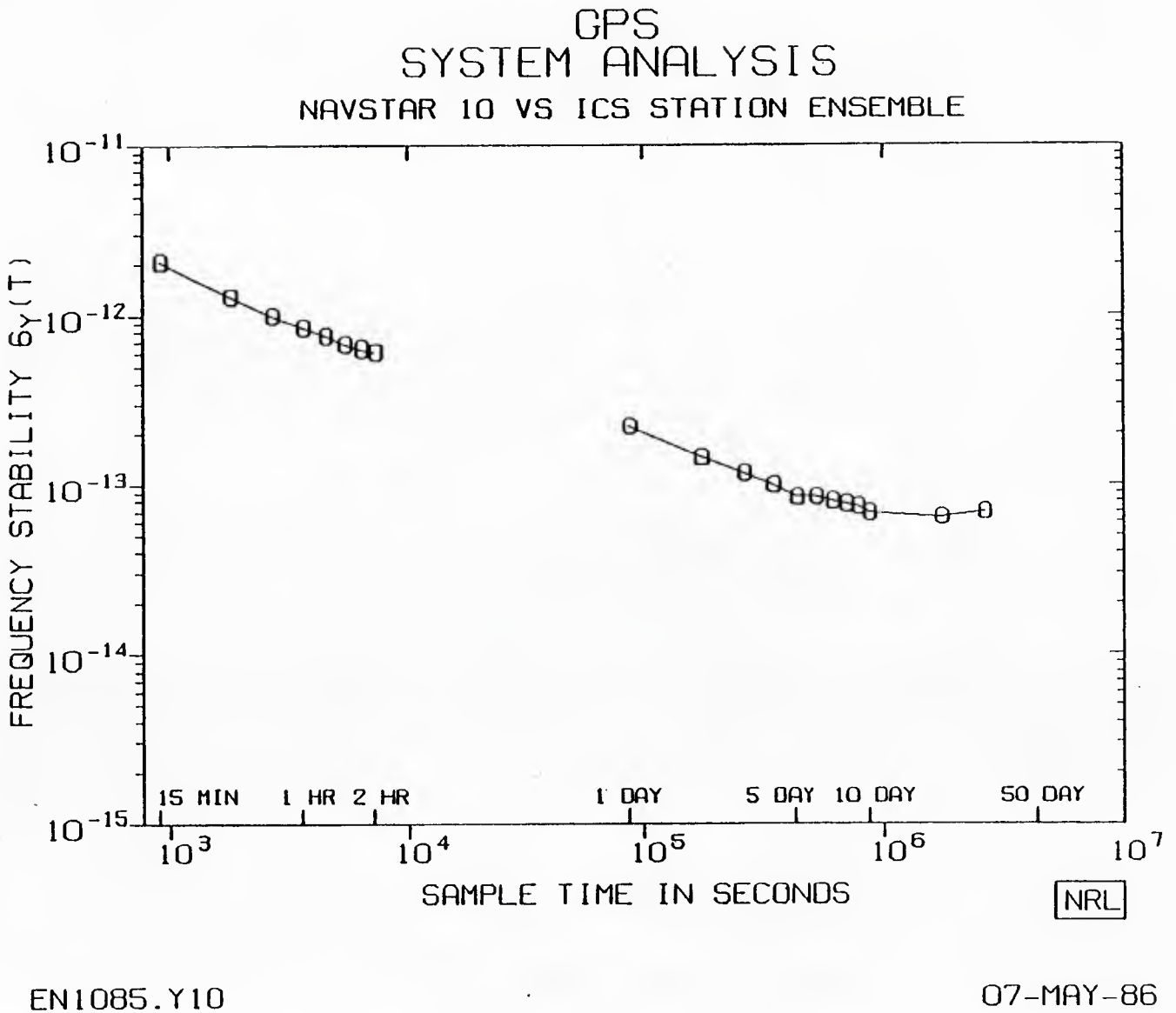
GPS
SYSTEM ANALYSIS
NAVSTAR 10 VS ICS STATION ENSEMBLE
FREQUENCY STABILITY σy(T)
10^-11
10^-12
10^-13
10^-14
10^-15
15 MIN
1 HR
2 HR
1 DAY
5 DAY
10 DAY
50 DAY
10^3
10^4
10^5
10^6
10^7
SAMPLE TIME IN SECONDS
NRL
EN1085.Y10
07-MAY-86

Figure 24

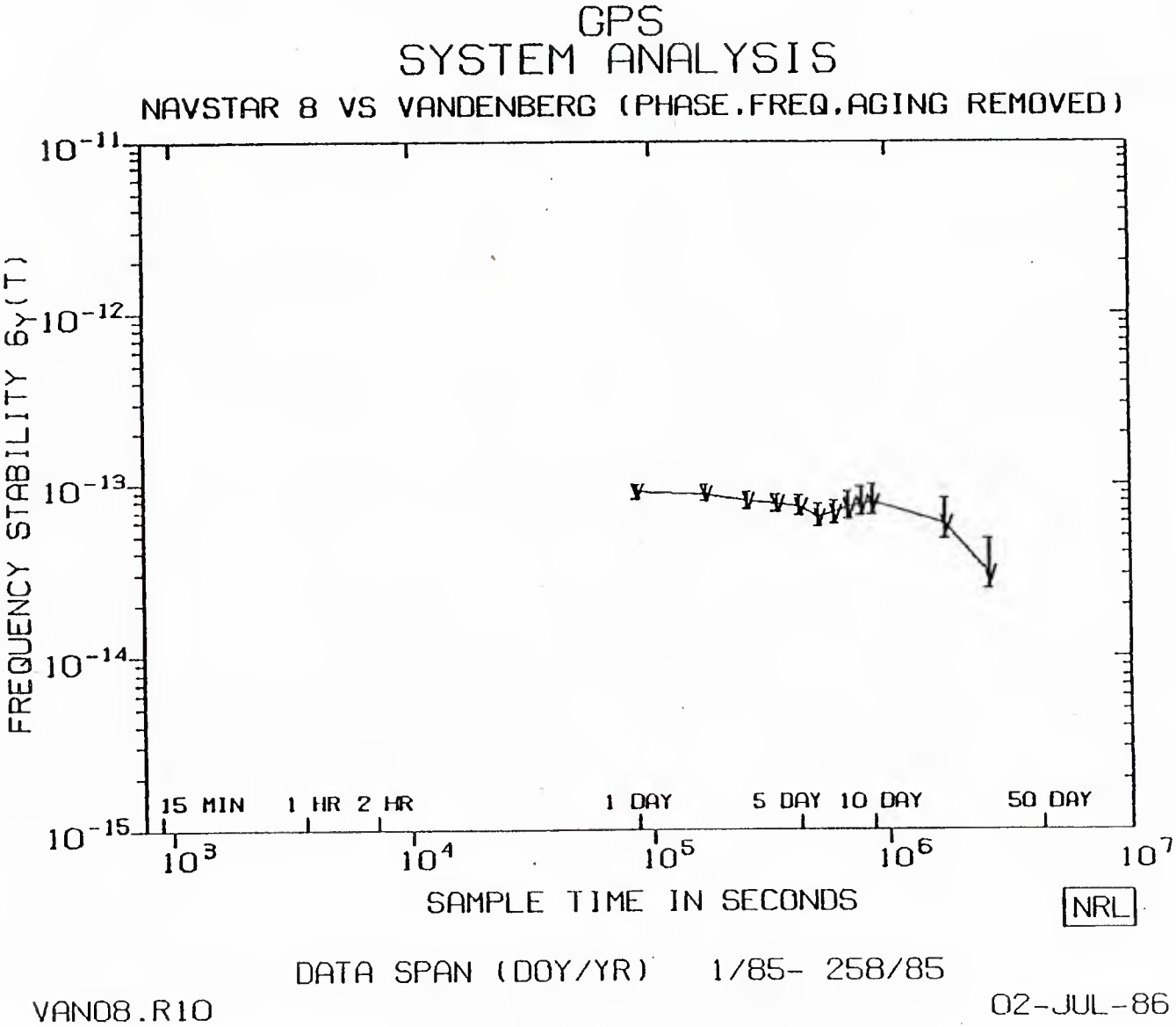
GPS
SYSTEM ANALYSIS
NAVSTAR 8 VS VANDENBERG (PHASE,FREQ,AGING REMOVED)
FREQUENCY STABILITY σy(T)
10^-11
10^-12
10^-13
10^-14
10^-15
15 MIN
1 HR
2 HR
1 DAY
5 DAY
10 DAY
50 DAY
10^3
10^4
10^5
10^6
10^7
SAMPLE TIME IN SECONDS
NRL
DATA SPAN (DOY/YR) 1/85- 258/85
VAN08.R10
02-JUL-86

Figure 25

GPS SYSTEM CLOCK ANALYSIS

PARAMETER	NRL	USNO
FREQUENCY	DUAL	L1 ONLY
GROUND CLOCK	SINGLE MS CESIUM	ENSEMBLE UTC (USNO)
SATELLITE EPHEMERIS	NSWC BEST FIT	PREDICTED NAV MESSAGE
DATA RATE/PASS	TCA 15 MIN SMOOTHED	13 MIN SMOOTHED SINGLE POINT
TRACKING STATION	4 GPS MS VAN, GUAM, HAW, ALA	USNO
SAMPLE AVERAGING TIMES	15 MIN - 2 HOURS 1 DAY - 100 DAYS	1 DAY - 64 DAYS

Figure 26

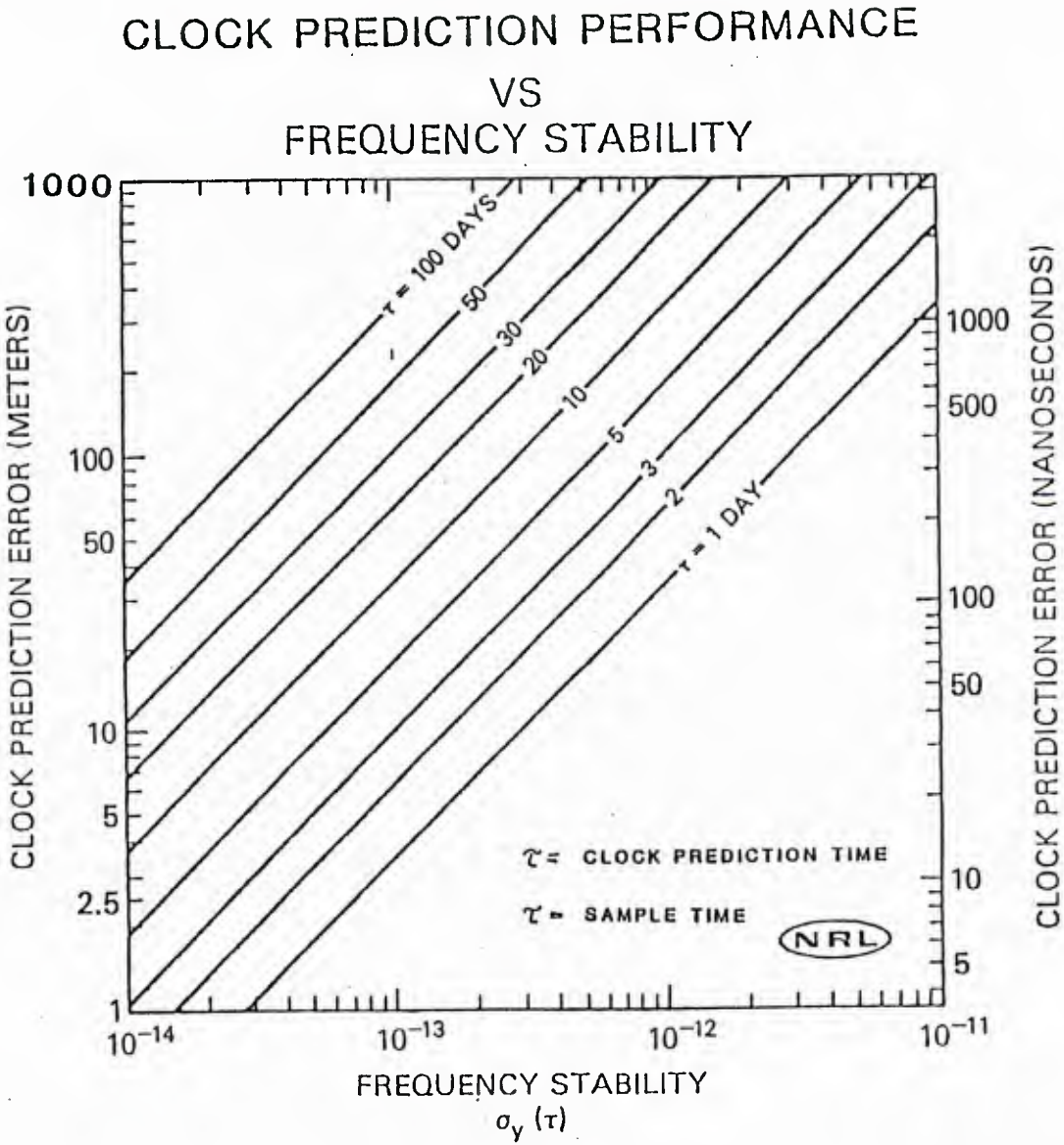
CLOCK PREDICTION PERFORMANCE
VS
FREQUENCY STABILITY
1000
100
50
10
5
2.5
1
τ = 100 DAYS
50
30
20
10
5
3
2
τ = 1 DAY
τ = CLOCK PREDICTION TIME
τ = SAMPLE TIME
NRL
CLOCK PREDICTION ERROR (METERS)
1000
500
100
50
10
5
CLOCK PREDICTION ERROR (NANOSECONDS)
10^-14
10^-13
10^-12
10^-11
FREQUENCY STABILITY
σy (τ)

Figure 27

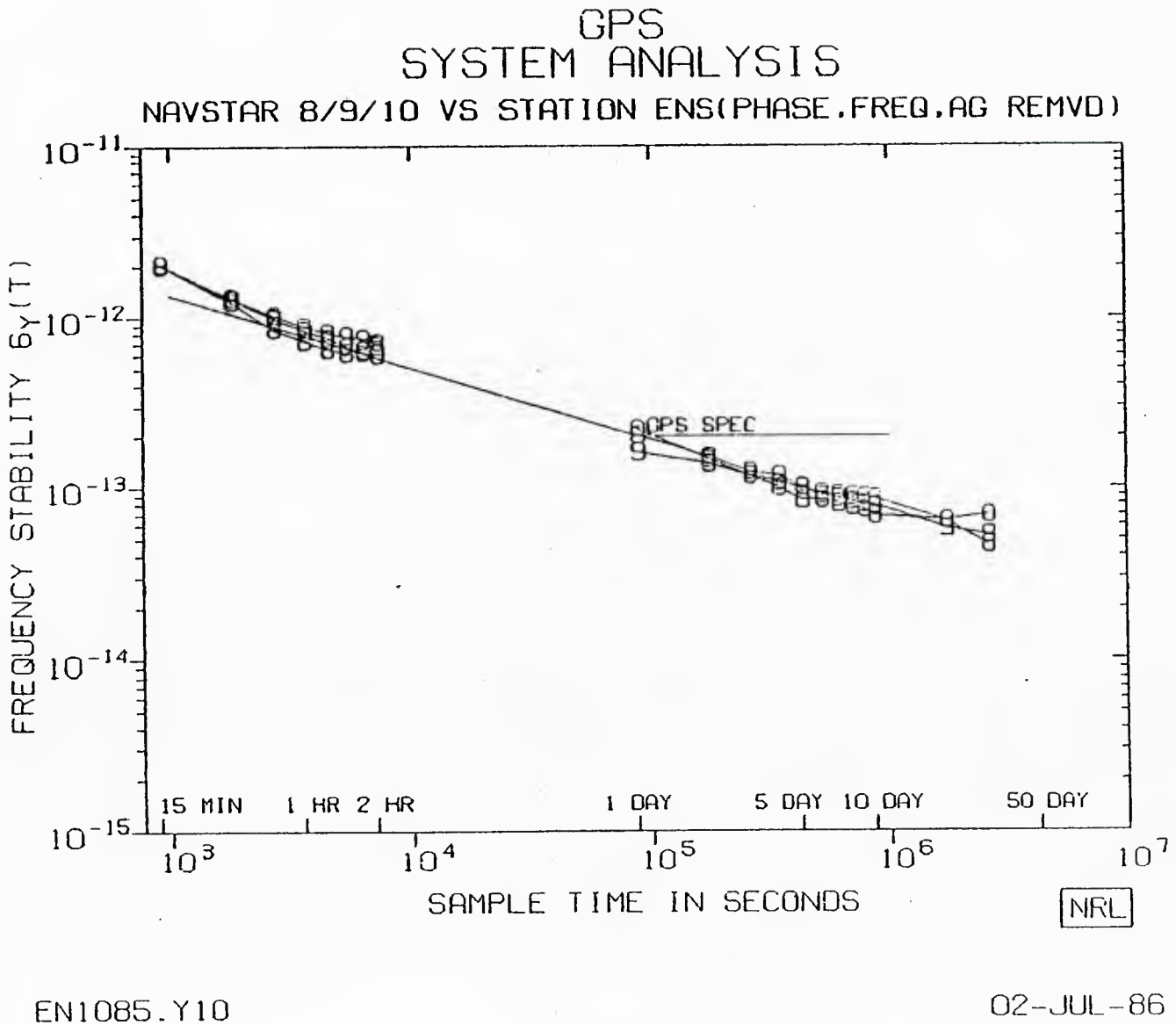
GPS
SYSTEM ANALYSIS
NAVSTAR 8/9/10 VS STATION ENS(PHASE.FREQ.AG REMVD)
FREQUENCY STABILITY σy(T)
10^-11
10^-12
10^-13
10^-14
10^-15
GPS SPEC
15 MIN
1 HR
2 HR
1 DAY
5 DAY
10 DAY
50 DAY
10^3
10^4
10^5
10^6
10^7
SAMPLE TIME IN SECONDS
NRL
EN1085.Y10
02-JUL-86

Figure 28

DEPARTMENT OF THE NAVY

NAVAL RESEARCH LABORATORY
Washington, D.C. 20375-5000

OFFICIAL BUSINESS
PENALTY FOR PRIVATE USE, $300